Chapter 19

BODIPY Laser dyes applied in sensing and monitoring environmental properties

Jorge Bañuelos *, Fernando Lopez Arbeloa, Teresa Arbeloa, Virginia Martinez, and Iñigo López Arbeloa

Departamento de Química Física, Universidad del País Vasco UPV / EHU, Apartado 644, 48080-Bilbao, Spain (* Corresponding Author, Phone : +34-946012711, Fax : +34-946013500, E mail : jorge.banuelos@ehu.es).

Content :

1. Introduction :

Fluorescent dyes have been intensively studied by the scientific community in multidisciplinary areas. The technological interest of these dyes has allowed their successfully application as active media of tunable lasers, in the development of photoelectronic devices, as fluorescent probes and chemical sensor, or monitoring the physicochemical characteristics of the surrounding ambiences [1 – 7]. The understanding of the photophysical properties of these systems is of capital importance, not only because of the intrinsic potential applications but also in the design of new dyes with specific properties. Indeed, a satisfactory correlation between the photophysical properties and lasing characteristics of several laser dyes has been established [8 – 16] by changing the molecular structure of the chromophore (substituent effect) and the environmental conditions (solvent effect, incorporation in rigid sold materials, etc).

Among the large number of existing laser dye families covering the spectral region from UV to near–IR [1], difluoro–boraindacene or boron–dipyrromethene complexes (BODIPY) have received special attention. Their basic structure, depicted in Scheme 1, consists in two pyrrole rings linked by a methene and a BF_2 groups. The first report related with these dyes dates from 1968 by Treibs and Keuzer [17], but they do not gain recognition from the scientific community until the end of nineties when some reports by Boyer and Pavlopoulos shown their potential application in tunable lasers [18 – 21]. The promising results obtained encourage to other researches to get a deeper inside in their lasing behaviour and to use this dye family in other fields such as biology or medicine [22 – 26]. Indeed, a huge number of publications arisen in a short time period describing their properties and applications [27 – 30].

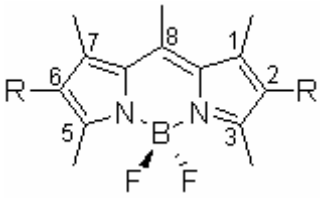

BODIPY	R
PM546	H
PM567	C_2H_5
PM597	$C(CH_3)_3$

Scheme (1) : Alkyl substituted BODIPYs.

BODIPY laser dyes present strong absorption and fluorescence bands in the visible spectral region, giving high fluorescent [31 – 38] and lasing efficiencies [18 – 21, 39 – 41]. Besides, their versatility, chemical robustness, low triplet state population, thermal and photochemical stability enhance the photoresponse of these dyes. For instance, highly efficient lasing signals after multitude of pumping pulses can be achieved when the BODIPY dyes are incorporated in solid host matrices [42 – 48]. This facilitates the development of solid–state tunable dye lasers, with important advantages with respect liquid–state lasers such as better manageability, versatility and miniaturization of the experimental set up, and the lack of toxic and flammable solvents [47, 48].

On the other hand, a large number of publications have claimed the use of BODIPY dyes in different photoelectronic devices: for instance as light harvesting arrays and antenna systems [49 – 53], acting as energy injector or acceptor to collect light and to carry it to a specific reaction centre; or in holographic systems for digital information storage [54 – 56]. Moreover, many reports have described the use of BODIPYs as fluorescent probes or chemical sensors in biomedicine and biochemistry. In these cases, the photophysics of BODIPYs have to be sensitive to the environmental properties [57 – 61] or to the presence of an analyte in the surrounding medium [62 – 72]. Usually, these probes or sensors are general achieved by the incorporation of specific functional groups in the BOIDIPY core, promoting new deactivation processes sensitive to environmental conditions (*i.e.*, photoinduced charge transfer). These processes quench the fluorescence of the dye, and the sensor behaves as a fluorescent on/off switch system depending of the environmental conditions.

The knowledge of the photophysical behaviour of BODIPY dyes is essential to understand their lasing action and to design new photoelectronic sensors or devices based on BODIPYs. Apart of experimental studies, quantum mechanical calculations have become a powerful tool to design new molecular structures with specific photophysical properties [73 – 77]. This chapter summarizes the photophysics of BODIPY dyes studied by our research group in the last few years. The experimental results are complimented by quantum mechanic calculation results. The influence of structural (substituent effect) and environmental (dye concentration, temperature, nature of the solvent, rigidity of the polymeric matrix …) factors are analyzed. Thus, the incorporation of electron donating (amino or acetamido) and accepting (cyano) groups can provide important changes in the photophysical properties of the chromophore (red–shifted absorption and fluorescence bands and solvent–polarity charge transfer phenomena). Besides, multichromophoric polyphenylene–BODIPY systems lead to intramolecular energy transfer processes, extended to the UV the spectral region for the photoactivity of BODIPYs.

2. General photophysics of BODIPY dyes :

The typical UV/Vis absorption and fluorescence spectra of BODIPYs are shown in Figure (1). The lowest energy Vis absorption band, corresponding to the electronic transition from the ground to the first excited states ($S_0 \rightarrow S_1$ transition), is characterized by a high transition probability, with high molar absorption coefficient ($\varepsilon \sim 10^5$ M^{-1} cm^{-1}) and oscillator strength ($f \approx 0.5$). It presents a shoulder at higher energies (at around 1100 cm^{-1} from the absorption maximum), which is attributed to out–of–plane vibrations of the aromatic skeleton. Other absorption bands, corresponding to transitions to higher singlet excited states (S_2, S_3…), appear in the UV region and are less probable [27, 78]. Quantum mechanical calculations suggest that the main absorption band corresponds to an allowed $A_1 \rightarrow B_2$ transition for the unsubstituted chromophoric system, characterized with a C_{2v} symmetry. Theoretical results indicate that this Vis band is assignable to the promotion of an electron from the HOMO orbital to the LUMO molecular orbital (Figure 1A), which is polarized along the long molecular axis of the chromophore [79].

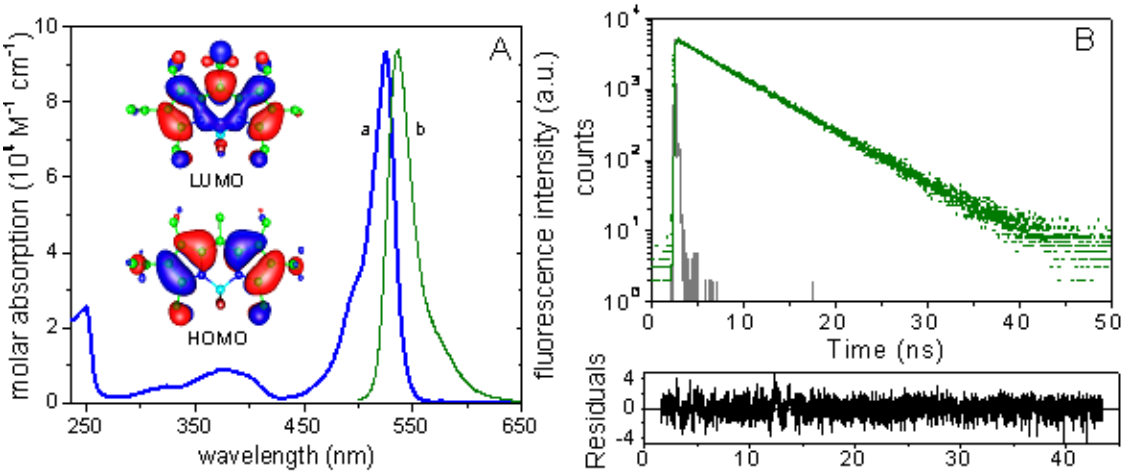

Figure (1) : (A) Absorption (a) and fluorescence (b) spectra and (B) fluorescence decay curve (top) and residuals.(bottom) of PM567 in diluted solutions (2×10^{-6} M) of c–hexane [78].

The shape of this absorption band is nearly independent of the dye concentration (at least up to 2×10^{-3} M) suggesting the absence of any intermolecular dye–dye interaction, including dye aggregation [27]. This low tendency of BODIPYs to self–associate is a very important advantage of these dyes with respect to other laser dyes, such as rhodamines, since the formation of non– or poorly fluorescent aggregates, drastically reduces the fluorescent capacity in concentrated solutions, generally required to record the laser signal [16].

The fluorescence spectrum of BODIPYs is practically the mirror image of the $S_0 \rightarrow S_1$ absorption band (Figure 1A), suggesting similar vibrational levels in both electronic states. Indeed, quantum mechanical calculations point out that the optimised geometry in the S_1 excited state is quite similar to that of the S_0 ground state. Consequently, the fluorescent band is characterized by a small Stokes shift in the rage of 500 cm^{-1}. The shape of the fluorescence band is independent of the excitation wavelength indicating that the emission is from the lowest vibrational level of the S_1 excited state, independent of the electron–vibrational level directly populated in the excitation process [27]. Therefore, a very fast internal conversion process from upper excited states populates the fluorescent excited state. The fluorescence quantum yield (ϕ) can be very high, reaching values close to the unit for some BODIPYs in certain media [27, 78].

Generally, the fluorescence decay curves of BODIPYs can be analyzed as monoexpoenential decays, with fluorescence lifetimes (τ) around 4–6 ns (Figure 1B). The lifetime is independent of the excitation and the emission wavelengths, confirming the simple emission from the locally excited state [27].

The high fluorescence ability of BODIPY is a consequence of its chromophoric unit. The BF_2 group acts as a linking bridge, providing a rigid delocalized π–system. The BF_2 group does not participate in the aromaticity of the π–system but avoids any cyclic electron flow around the chromophoric ring [80]. Consequently, BODIPY dyes can be classified as quasi–aromatic dyes and are characterized by a low intersystem crossing probability by means of the "Drexhage's loop rule" [2]. This low population of the triplet state [81] is a significant advantage for the potential application of BODIPYs in photonics since the triplet–triplet absorption, one of the most important losses in the resonator cavity, is drastically reduced. Therefore the non–radiative deactivation pathways are mainly controlled by internal conversion processes. In any case, and due to the rigidity and planarity of the chromophoric units (confirmed by quantum mechanical calculations and X–ray diffraction data [79, 82]), the non–radiative deactivation of BODIPY dyes is expected to be low, in agreement with the experimental evidences for the high fluorescence ability of these dyes [2, 27, 83].

The fluorescent band and decay curves of BODIPY dyes present an important dependence on the dye concentration. Indeed, an augmentation in the optical density of the samples leads to a bathochromic shift in the fluorescent band, an important decrease of its intensity and an augmentation of the lifetime [16]. These effects are attributed to inner filter effect (*i.e*. reabsorption/reemission phenomena) rather than to any intermolecular dye–dye interaction affecting the emission characteristics (*i.e.* excimer formation). Indeed, the photophysical properties recorded at high dye concentrations return to the original values obtained in diluted dye samples when the fluorescent signals were registered in the front–face configuration with very narrow optical pathway cuvettes (0.001 cm) [84]. The reabsorption/reemission effects observed in moderated

optical density samples (for instance in solid polymeric matrices) can be corrected by mathematical procedures [85].

2.1 Effects of 2- and 6-Alkyl groups :

The experimental and theoretically predicted photophysical properties of commercially PM546 [86], PM567 [78] and PM597 [87] alkyl−BODIPY dyes in a common apolar solvent are summarized in Table (1). All these dyes present methyl groups at 1, 3, 5, 7 and 8 positions of the chomophoric ring, and PM567 and PM597 derivatives present ethyl and *tert*–butyl groups, respectively, at 2 and 6 positions (Scheme 1). The experimental results suggest that the ethyl groups do not significant affect on the photophysics of BODIPY chromophore [78]. For instance, the absorption and fluorescence bands of PM567 are bathochromically shifted around 25 nm with respect to the spectral bands of PM546, with similar fluorescence quantum yields and lifetimes. However, the presence of the *tert*−butyl groups (PM597) not only induces further bathochromic spectral shifts, mainly in the fluorescence band (around 55 nm), but also decreases the fluorescence quantum yield and lifetime, with values around half to those obtained for the PM546 dye [87]. These results reveal an important Stokes shift (around 1300 cm^{-1}) and a considerable increase in the non–radiative rate constant (k_{nr}) of PM597 with respect to the other PM546 and PM567 dyes (Table 1).

Table (1) : Experimental and theoretically predicted (TD–B3LYP in gas phase) photophysical properties of alkyl−BODIPYs (PM546 [79,86], PM567 [78,88] and PM597 [87]): wavelength of absorption and fluorescence maximum (λ_{ab} and λ_{fl}), Stokes shift ($\Delta\nu_{St}$), molar absorption coefficient (ε_{max}), oscillator strength (f), fluorescence quantum yield (ϕ) and lifetime (τ), rate constants of radiative (k_{fl}) and non–radiative (k_{nr}) deactivation.

	Experimental *			Theoretical		
	PM546	PM567	PM597	PM546	PM567	PM597
λ_{ab} (± 0.2 nm)	492.0	516.2	523.0	403	426	429
ε_{max} (10^4 M^{-1} cm^{-1})	8.2	7.9	7.6	–	–	–
f	0.40	0.49	0.38	0.53	0.54	0.52
λ_{fl} (± 0.2 nm)	504.0	531.6	561.0	407	433	455
ϕ (± 0.05)	0.95	0.91	0.48	–	–	–
τ (± 0.1 ns)	5.58	6.10	4.21	–	–	–
k_{fl} (10^8 s^{-1})	1.71	1.49	1.14	1.88	1.60	1.61
k_{nr} (10^8 s^{-1})	0.09	0.15	1.23	–	–	–
$\Delta\nu_{St}$ (cm^{-1})	455	560	1305	215	360	1365

* dye concentration (2×10^{-6} M) in methanol

These experimental tendencies are theoretical predicted by quantum mechanical calculations. It was previously demonstrated that the absolute S_0–S_1 energy gap values proposed by semiempirical methods are closer to the experimental ones than those predicted by the TD–B3LYP method. Indeed, this DFT method overestimates this energy gap. However, the DFT method provides better values for the oscillator strength (f) and the radiative rate constant (k_{fl}) and reproduces more accurately the spectral shifts and changes in the transition moments of

BODIPYs by the effect of the substituents and the solvent. Fir this reason, the DFT results are enclosed in Table (1) [79, 88].

The observed bathochromic spectral shifts by the presence of alkyl groups at the 2 and 6 positions can be interpreted in terms of the inductive effect. Quantum mechanical calculations suggest a lower electron density at the 2 and 6 positions in the LUMO than in the HOMO state (see contour maps inserted in Figure 1). Consequently, the inductive effect +I of alkyl group at the 2– and 6–position would stabilize more extensively the LUMO S_1 excited state than the HOMO S_0 ground state, reducing the S_0–S_1 energy gap (spectral shift to lower energies). Because the inductive effect +I of the branched *tert*–butyl group is higher than that of the ethyl group, the bathochromic shift is more significant in the PM597 than in the PM567 derivative (Table 1) [87].

For PM597, the bathochromic shift in the fluorescence band is higher than in the absorption band giving rise to a large Stokes shift (Table 1). This observation could be indicative of a change in the geometry of this derivative upon excitation. This is confirmed by quantum mechanical calculations. Indeed, the pyrrole rings are not planar in the S_1 excited state of PM597 (dihedral angle of 4.7º) versus the nearly planar structure (dihedral angle around 0.2º) proposed for the pyrrole ring in the S_1 state of PM567. This distortion in the S_1 geometry has been attributed to the steric hindrance between the bulky *tert*–butyl groups with the adjacent methyl groups at 1– and 7–position of the PM597 core [87]. This loss in the planarity can be interpreted as a reduction in the rigidity of the chromophoric BODIPY system, favouring the internal conversion processes for PM597 and reducing its fluorescent capacity with respect to other BODIPY dyes with linear alkyl groups (Table 1) [87].

2.2 Solvent Effect :

The photophysical properties of alkyl–BODIPY dyes have been studied in a wide variety of apolar, polar and protic solvents [87]. The corresponding results for PM597 dye are summarized in Table (2). Other alkyl–BODIPYs show similar qualitative tendencies [78, 86]. In general, the spectral bands shift to higher energies and the fluorescent capacity and lifetime increase when apolar media are changed by polar/protic media. The augmentation in the fluorescence ability is due to a reduction in the non–radiative deactivation rather than to an enhancement in the radiative decay [83]. All these experimental results have been confirmed by quantum mechanics [79, 88].

The alternating electronic charge delocalisation through the conjugated π–system suggests that BODIPY dyes can be defined as cyclic polymethine– or cyanine–like structures [89, 90]. The dipole moment, oriented along the short molecular axis due to symmetry reasons, is relatively low ($\mu \approx 3$ D in the ground state), making BODIPY dyes insoluble in water (except in those systems with charged substituents, *i.e*. PM556). Theoretical results suggest that the dipole moment slightly decrease upon excitation ($\Delta\mu = -1$ D in gas phase) [88]. Consequently, S_0 state would be more stable than S_1 one in polar solvents, giving rise to a moderate hypsochromic spectral shift with the solvent polarity, as is experimentally observed (Table 2). However, other solvent properties can affect the spectral bands.

Table (2) : Photophysics of PM597 dye in diluted solutions (2×10^{-6} M) of several solvents [87]

	Solvent	λ_{ab} (nm)	ε_{max} ($10^4 M^{-1}cm^{-1}$)	λ_{fl} (nm)	ϕ	τ (ns)
1	2–methylbutane	527.1	8.20	569.0	0.40	4.19
2	hexane	527.5	8.25	567.8	0.43	4.35
3	c–hexane	529.0	8.10	571.2	0.32	3.91
4	isooctane	527.5	8.05	569.0	0.40	4.43
5	diethyl ether	525.1	7.90	565.4	0.43	4.27
6	1,4–dioxane	525.1	7.85	565.4	0.40	4.37
7	THF*	525.1	7.75	566.6	0.37	4.15
8	DMF*	524.0	5.89	565.4	0.35	4.69
9	acetone	522.5	7.44	563.6	0.44	4.34
10	2–pentanone	523.7	6.13	562.6	0.46	4.54
11	methyl formate	522.3	7.55	560.6	0.47	4.45
12	methyl acetate	522.5	7.85	561.8	0.48	4.44
13	ethyl acetate	523.2	7.67	562.4	0.44	4.31
14	buthyl acetate	524.3	7.85	564.6	0.43	4.51
15	acetonitrile	520.8	7.60	560.6	0.44	4.27
16	1–octanol	527.3	7.70	565.0	0.41	4.68
17	1–hexanol	526.7	7.55	565.4	0.42	4.59
18	1–butanol	526.1	7.70	566.6	0.39	4.33
19	1–propanol	525.3	7.75	564.6	0.39	4.19
20	ethanol	524.3	7.63	563.2	0.43	4.09
21	methanol	522.9	7.58	561.2	0.48	4.21
22	F3–ethanol*	521.6	7.01	561.2	0.49	4.64

*DMF = dimethylformamide, THF = tetrahidrofurane, F3-ethanol=2,2,2–trifluoroethanol

An accurate understanding of the solvent effect can be achieved by a multilinear correlation analysis [91, 92]. This method is based on the fact that a physicochemical property (XYZ) can be simultaneously correlated by a linear relationship with different solvent parameters (A, B, C, ..) by means of -

$$(XYZ) = (XYZ)_o + c_A A + c_B B + c_C C + \ldots. \quad (1)$$

where $(XYZ)_o$ is the physicochemical property of interest in an inert solvent and c_A, c_B, c_C, … are the adjusted coefficients, which reflect the dependence of the physicochemical property on the corresponding A, B, C,…. solvent parameters.

The photophysical properties of aromatic system are generally correlated with the solvent polarity/polarizability, H–bond donor / acceptor capacity and electron releasing ability [91]. The solvent properties can be described by the Taft π*–, α– and β–scales, respectively [93 – 95]. Figure (2) shows the evolution of the experimental absorption and emission maxima (ν_{ab} and ν_{fl} in cm^{-1}) of PM597 [87] with those best predicted from the adjustable equation (1). The random distribution of the experimental data with the predicted values confirm the validity of adjustable method from which the adjusted c_{π^*}, c_α and c_β coefficients can be evaluated. These values are included in the respective graphs (Figure 2). The relative low correlation coefficient ($r < 0.9$) is due to the relative low spectral shifts observed for PM597 from apolar to very polar/protic solvents (not more than 10 nm). The c_{π^*}, c_α and c_β coefficients can be compared each other if the range values of π*, α and β parameters from apolar to polar/protic solvents reach similar intervals, as is the present case with π*–, α– and β–scales in the approximately 0 – 1 range. Experimental results suggest that the absorption and fluorescence bands of PM597 are mainly affected by the solvent polarity / polarizability (high c_{π^*} values), although the electron release capacity of the solvent can also affect, in some extent, on the band position. In general absorption and fluorescence bands shift to higher energies by increasing the solvent polarity/polarizability ($c_{\pi^*} > 0$), while the solvent basicity induces slight spectral shifts toward lower energies ($c_\beta \leq 0$). The effect of the solvent acidity on the spectral positions is practically neglectable ($c_\alpha \approx 0$), mainly in the absorption band.

An alternative method to analyze the solvent effect on the spectroscopic parameters is by means of a linear relationship between a physicochemical properties (XYZ) and a multicomponent solvent parameter (M), equation (2), in which several solvent properties are included [92].

$$(XYZ) = (XYZ)_o + c_M M \qquad (2)$$

For instance, the Reichardt $E_T^N(30)$ is a very popular multicomponent solvent parameter in which both solvent polarity/polarizability and H–bond capacities are included [96].

The observed increase in the ϕ and τ values of PM597 with the solvent polarity (Table 2), is mainly due to a decrease in the k_{nr} rate constant rather than to an increase in the k_{fl} value which is observed to be nearly solvent independent [87]. Figure (3) shows the evolution of the k_{nr} value (in logarithm scale) of PM597 with the $E_T^N(30)$ solvent parameter. The good linear relationship ($r = 0.85–0.90$) suggest the validity of equation (2) applicable, in this case, for the non–radiative deactivation rate constant of PM597. The reduction of the internal conversion in polar/protic solvents could be due to a diminution of the electron flow as a consequence of a restriction in the delocalization of the positive charge through the π–system of the BODIPY chromophore [83]. Previous works of rhodamines and coumarins demonstrated that those factors favouring the movement of the positive charge through the delocalized π–system can be look as a loss in the rigidity of the chromophoric system and hence to a decrease of the fluorescence ability [11]. Thus, an electrostatic stabilization of the positive charge with the dielectric

constant of the solvent or any specific solute–solvent interaction reducing the charge mobility through the conjugated π–system, should lead to a diminution in the non–radiative deactivation. Similar arguments can be applied for the case of other alkyl–BODIPY dyes [32, 78, 86].

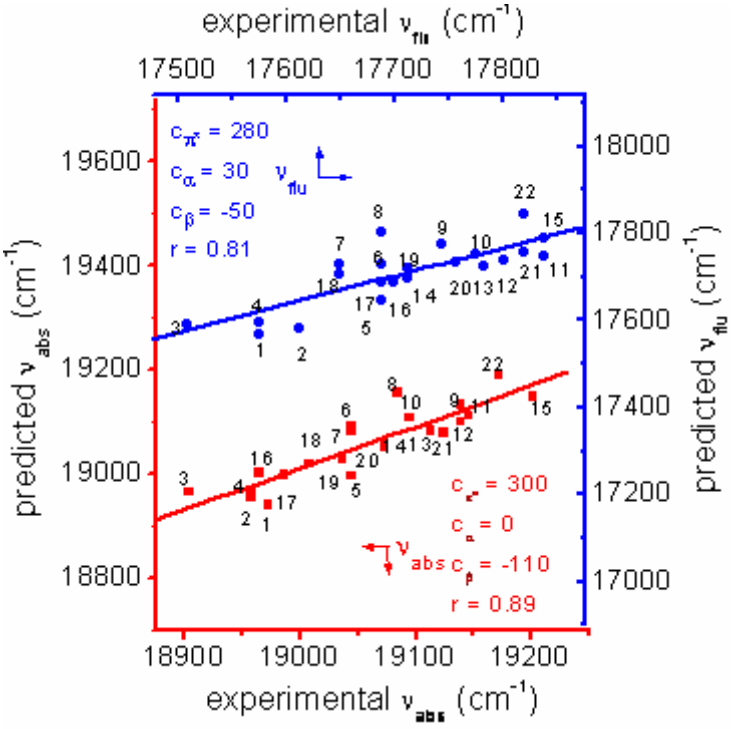

Figure (2) : Multiple linear regression of the absorption and fluorescence wavenumber of PM597 [87] in a wide variety of media using the Taft solvent scales [87]: apolar (1–4), polar/aprotic (5–15) and polar/protic (16–22) solvents (see Table 2).

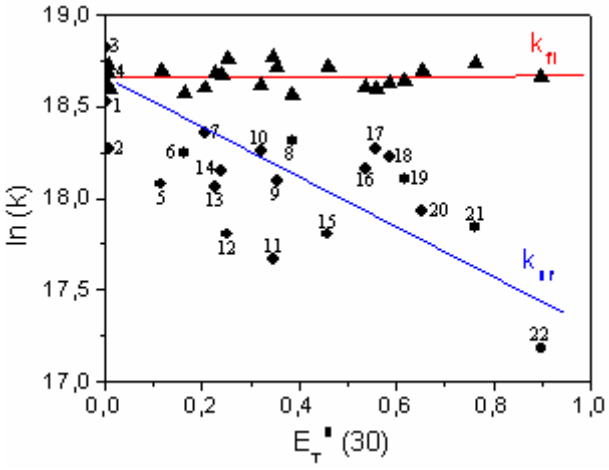

Figure (3) : Evolution of the radiative (k_{fl}) and non-raditative (k_{nr}) deactivation rate constants of PM597 with the Reichardt solvent parameter $E_T^N(30)$ [87].

It has been previously proven a good correlation between the photophysical properties and the lasing characteristics of alkyl–BODIPYs by changing both the molecular structure of the dye (substituent effect) and the solvent [84, 97]. Thus, similar bathochromic spectral shifts are observed in the fluorescence and lasing band by the incorporation of ethyl (PM567) or *tert*–butyl (PM597) groups at the 2– and 6–positions of PM546 or changing from a polar/protic solvent to an apolar environment for a common alkyl–BODIPY dye (PM546, PM567 or PM597). Similar correlation can be also established between the lasing efficiency and the fluorescence capacity by changing both the molecular structure of the dye and the environmental conditions of the surrounding media.

2.3 Photophysics of BODIPYs in solid polymeric matrices :

The recent innovations in tunable lasers are being oriented to the development of solid–state dye lasers. They have interesting technological advantages such as the compactness, the absence of toxic and inflammable solvents, etc. In these lasers, the dye is embedded into a transparent solid host material, which can be of both organic and inorganic nature [47, 48]. Inorganic materials generally improve the mechanical and thermal stability of the active media, whereas organic materials favour the chemical compatibility between the host and the guest materials. One of the most commonly used organic host matrices are polymer systems. Concretely, polymethylmethacrylate (PMMA) has been largely used as organic host material because of the nice optical homogeneity and the viscoelastic properties and polarity of the polymer can be controlled by the synthesis conditions [98].

Alkyl–BODIPY dyes have been incorporated into PMMA matrices, both as dopant and covalently linked to the polymer chain [99 – 103]. Since the rigidity of molecular systems enhances the fluorescence capacity of BODIPYs, the elasticity/rigidity of the PMMA solid matrix can be modified by the copolymerization of MMA with adequate crosslinking agents [104]. Trifunctionalized methacrylate (TMPTMA) and tetrafunctionized acrylate (PETRA), shown in Scheme (2), were used for this purpose. On the other hand, and since the highest fluorescence capacity of BODIPYs have been obtained in trifluoroethanol as solvent Table 2, PM567 and PM597 have been incorporated not only into MMA but also into fluorinated–MMA copolymers [103]. Different fluorinated–MMA monomers (TFMA, PFMA and HFMA, in Scheme 2) and degrees of copolymerization have been considered. Finally, the covalent linkage of BODIPY core to PMMA chains can be performed by means of a polymerizable methacryloyloxy end group, which was incorporated in the *meso* 8−position of the BODIPY via a polymethylene chain (–(CH_2)n–, with n = 1, 3, 5, 10 and 15 methylene units, Scheme 2) or a *para* substituted phenyl group (Scheme 2) [99, 100, 102].

The photophysics of PM567 in PMMA with different crosslinking agents have been reported elsewhere [101]. In general, the experimental results indicate that the absorption and fluorescence bands practically do not shift with the solid matrix (similar λ_{ab} and λ_{fl} values are obtained in pure solid PMMA and in liquid ethanol, a solvent which can mimetic the physicochemical properties of MMA) neither with the nature and degree of the crosslinking agent. However, as is illustrated in Figure (4), the ϕ value of PM567 changes with the type and extent of the linking comonomers. Indeed there is an optimal crosslinking degree maximizing the fluorescence capacity of PM567, which depends on the nature of the crosslinking agent (around 10 % for

TMPTMA and around 1% for PETRA). Similar evolutions have been reported for the lasing efficiency (% Eff.) of PM567 [104], corroborating previous conclusions in the sense that those structural and environmental conditions optimizing the fluorescent emission of BODIPYs also improves the lasing efficiency.

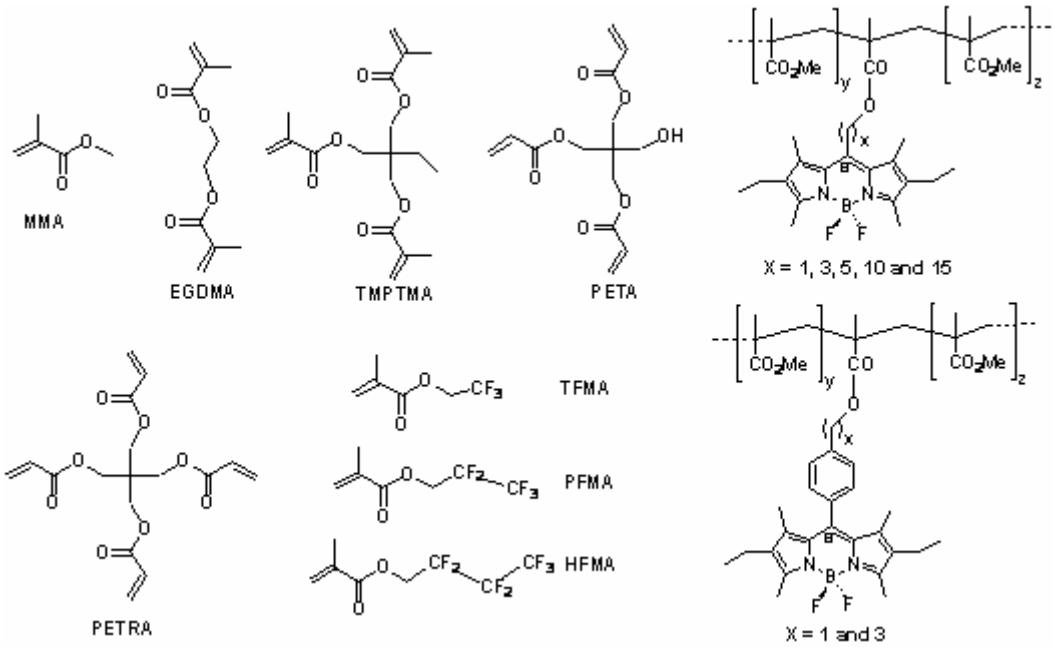

Scheme (2) : Molecular structure of the monomers and dye linkage to the PMMA chain trough a linear spacer of different length or by a *para* substituted phenyl groups [99,100, 102, 104].

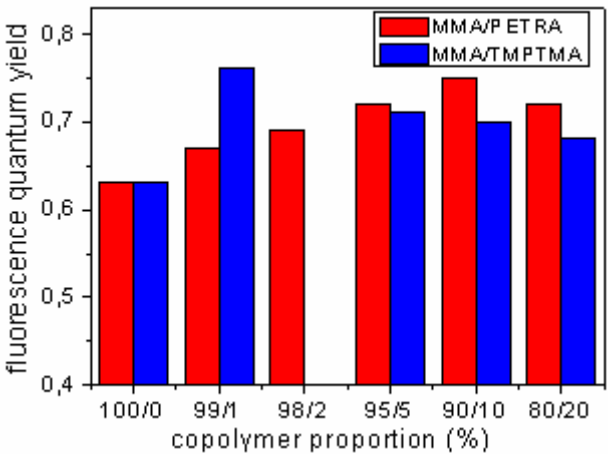

Figure (4) : Evolution of the fluorescence quantum yield of PM567 with the concentration of the crosslinling agent (PETRA and TMPTMA) in the copolymer with MMA [101].

This different behaviour with the crosslinking agent has been related to the glass transition temperature (T_g) of the copolymer matrix [104]. The T_g value of acrylic TMPTMA crosslinker is lower than that of the methacrylic PETRA one, providing a less rigid environment in the former case for the same crosslinking degree. In other words, the optimized rigidity of the polymer MMA matrix is reached for a lower PETRA crosslinker concentration than in the case of TMPTMA. A further increase in the crosslinking degree beyond this optimal point reduces the fluorescence capacity, probably because an excessively rigid environment damages the dye.

On the other hand, PM567 and PM597 have been incorporated in crosslinked fluorinated PMMA copolymers [103]. Figure (5) shows the evolution of the ϕ value of PM567 and PM597 with the type of copolymer. For PM567, the fluorescence efficiency increases in fluorinated matrices with respect to in the homopolymer PMMA. This increase correlates with a similar augmentation observed in the fluorescence lifetime, suggesting a reduction in internal conversion processes of PM567. This diminution in the k_{nr} value agrees with that observed in liquid solution (F_3-ethanol in Table 2) and corroborates above conclusions in the sense that polar environments increase the fluorescence capacity of alkyl–BODIPYs [27, 32]. Even more, a further increase in the fluorescence capacity of PM567 is observed when crosslinker monomers are also included in the fluorinated matrices (Figure 5). Therefore, a more polar and rigid environment ameliorates the fluorescence, and hence the lasing, of alkyl–BODIPYs [103].

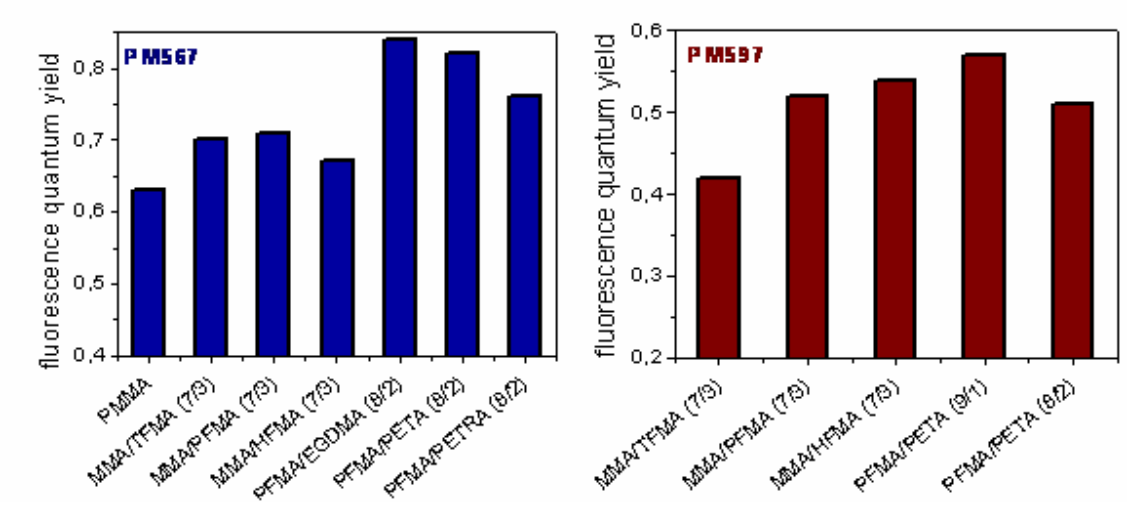

Figure (5) : Evolution of the fluorescence quantum yield of PM567 and PM597 with the type and proportion of fluorinated and crosslinked copolymers [103] (*nomenclature in Scheme 2*).

In the case of PM597 dye, the effect of the solid polymeric matrices is more pronounced. This dye presents higher fluorescence quantum yields and lifetimes in solid polymers ($\phi \approx 0.5 - 0.6$ and $\tau \approx 7 - 8$ ns) than in liquid solutions ($\phi \approx 0.4 - 0.5$ and $\tau \approx 4.0 - 4.5$ ns). As is discussed above, the internal conversion of PM597 is higher than other alkyl–BODIPY dyes due to a loss in the planarity of the chromophoric ring in the excited state [87]. Such a geometrical change could be reduced in the rigid environment provided by the polymeric matrices, improving the fluorescence capacity of this dye in solid materials. Moreover, the fluorescence capacity of

PM597 progressively increases with the polarity and rigidity of the copolymer (Figure 5), with a similar evolution to that observed for PM567.

It has been proven that the photophysical properties of alkyl–BODIPYs covalently bounded to PMMA chains by a long enough spacer (Scheme 2) are very similar to the respective dyes incorporated in PMMA as dopants [99, 102]. Consequently, the covalently linkage does not improve the fluorescence, and hence the lasing, ability of alkyl–BODIPYs [99]. However, when the spacer is just one methylene unit, the fluorescence capacity decreases, due to a decrease of the radiative rate constant, and the spectral bands shifts to lower energies. Probably, for a short enough spacer, the inductive electron withdrawing of the methacryloyloxy group reduces the aromaticity of the electronic π–system of the chromophore, leading to a diminution in the radiative deactivation probability and an augmentation in the S_0–S_1 energy gap [84]. In any case, when the linking polymethylene chain is long enough (more than 3 methylene units) the high fluorescence capacity of the BODIPY is recovered [99].

When the phenyl group acts as a spacer between the polymer chain and the dye, the photophysical properties of BODIPYs are practically unaltered [100]. Quantum mechanical calculations reveal that the phenyl group is disposed practically perpendicular to the BODIPY core, avoiding any resonant interactions between the electronic clouds of both entities [83]. This perpendicular arrangement is assigned to the steric hindrance between the *ortho* H–atoms of the phenyl group and the adjacent methyl groups at the 1– and 7–position of the BODIPY core. Indeed, if these positions are unsubstituted, then the phenyl group at 8–position can be disposed coplanar with the BODIPY ring leading to important changes in the photophysics of the BODIPY chromophore, mainly with a decrease in the fluorescence capacity [105 – 108].

Therefore, if the covalent binding of the chromophore to the PMMA chain is carried out by a long enough linear polymethylene chain or a phenyl group, then the high fluorescence capacity of BODIPY is kept. Thus, the lasing efficiency of alkyl–BODIPYs does not change with the covalently linkage of the dye to the polymer chain [99, 102]. However, this covalent bond considerably enhances the thermostability of the BODIPY chromophore, probably because the chemical linkage provides extra pathways to the dye to eliminate the excess of heat accumulated during the laser action [99]. This effect is more pronounced if the dye presents two polymerizable end groups in the same molecule. In this case the dye can act as a crosslinking agent between two polymeric chains [102]. This strategy is of great importance in the application of BODIPY dyes in solid state lasers, because the thermal degradation is one of the most important reasons for dye damage [47, 48]. In this way, the operative lifetime of the active media can be considerably increased by the covalent linkage.

In summary, photophysical measurements and quantum mechanical calculations have demonstrated to be a good strategy to look for the best structural and environmental conditions to optimize the lasing performance of alkyl–BODIPY dyes. Rigid systems (both from a structural point of view and from environmental restrictions) and polar media are recommended to reach these conditions optimising the laser action of alkyl–BODIPY dyes. The covalently linkage of these BODIPY cores to a polymeric PMMA chain does not alter the fluorescence and lasing efficiencies of the dye, but considerably improves the thermostability of the dye [99, 100, 102].

2.4 Red shifted BODIPYs :

The emission region of BODIPYs can be modulated by the incorporation of adequate functional groups in the chromophoric unit. Alkyl–BODIPYs typically emit in the green–yellow part of the Vis region. However, and due to the potential technological application of dye lasers in the red and near–IR regions, new red–shifted laser dyes based on BODIPY skeleton are now being synthesised by different research groups [109 – 114]. The aim is to extend the delocalization of the electronic π–systems of BODIPYs by conjugation with suitable substituents generally incorporated at the 3 and 5, or 8 positions of BODIPY core.

Thus, the presence of a styryl group at 3–position of the PM567 core, the so–called PMS derivative (inset in Figure 6) [115], induces drastic bathochromic shifts (around 50 nm) in the absorption and fluorescence bands with respect to the corresponding spectral bands of the parent PM567 dye, (Figure 6). This shift to lower energies is a consequence of the extension of the delocalized electronic π–system through the styryl group. In fact, the contour maps of the HOMO and LUMO electronic states of PMS obtained by quantum mechanical calculations (inset in Figure 6) reveal a conjugation of the electronic clouds of both moieties.

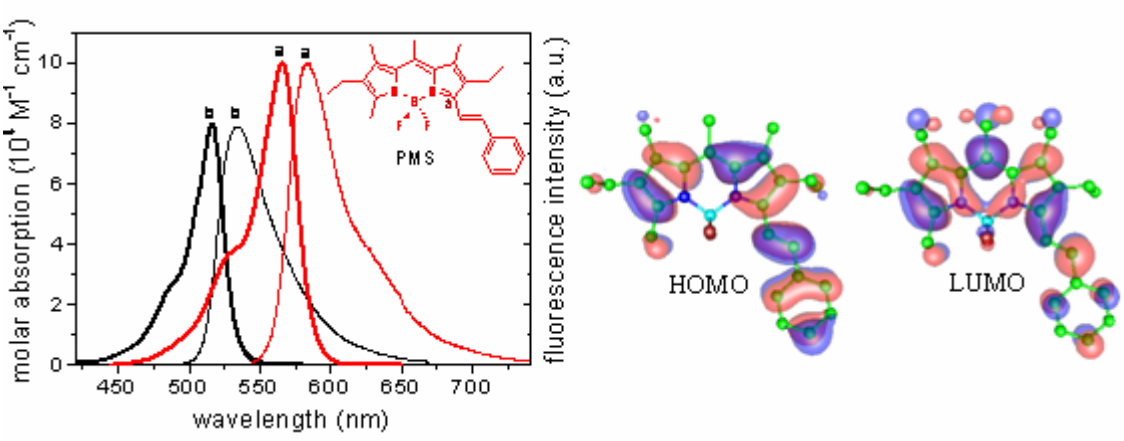

Figure (6) : Normalized absorption and fluorescence spectra of PMS (a) and PM567 (b) in diluted solutions of methanol [115]. The contour maps of the HOMO and LUMO of PMS are also included.

The extension in the π–system not only induces bathochromic shifts of the spectral bands but also leads to an augmentation of the S_0–S_1 spectroscopic transition probability, as is reflected in the molar absorption ε_{max} and oscillator strength f values of PMS (> 10^5 $M^{-1}cm^{-1}$ and 0.6 – 0.7, respectively), which are among the highest ones obtained up to now for BODIPY dyes. The fluorescence rate constant of PMS (k_{fl} = 1.53×10^8 s^{-1} in methanol) is also slightly higher than the corresponding value of PM567 (k_{fl} = 1.49×10^8 s^{-1}). However, PMS shows a somewhat lower fluorescence quantum yield and lifetime (ϕ = 0.82 and τ = 5.36 ns in methanol) than those values of PM567 (ϕ = 0.91 and τ = 6.10 ns) due to an augmentation in the non–radiative deactivation probability (from k_{nr} = 0.15×10^8 s^{-1} in PM567 to k_{nr} = 0.33×10^8 s^{-1} in PMS). This increase in the internal conversion of BODIPYs can be attributed to both a decrease in the

S_0–S_1 energy gap and/or an extra thermal dissipation of the excitation energy by the internal rotation and vibration movements of the styryl group. A possible non–radiative deactivation via a (*E*) → (*Z*) photoisomerization of the styryl double bond in the excited state [115] is discarded in the present case since only the (*E*) isomer of PMS is observed after prolonged visible light irradiation. The evolution of the photophysical properties of PMS with the nature of the solvent are similar to those above described for alkyl–BODIPYs (Section 2.1) [27, 32].

Red–shifted BODIPY dyes can be also achieved by incorporating electron donor groups at appropriated positions of the chromophoric ring [116, 117]. Thus, Figure (7) illustrates the presence of an acetamido group at 3–position of the BODIPY core induces moderate batho-chromic shifts (around 20 nm) in the absorption and fluorescence bands, with respect to the parent PM567 dye. These shifts are assigned to the augmentation in the delocalization of the electronic π–system through the acetamido group.

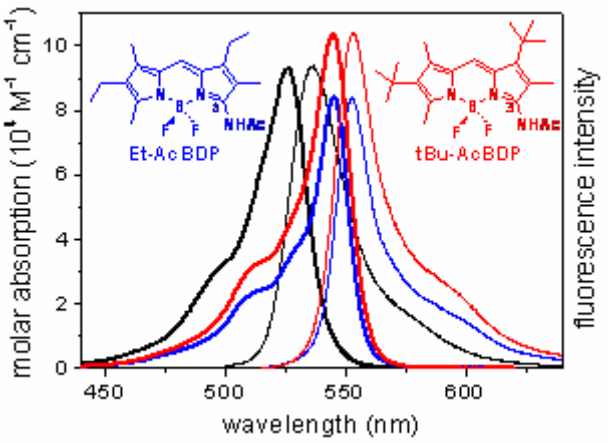

Figure (7) : Absorption and fluorescence spectra of 3–acetamido–BODIPYs; Et–AcBDP and tBu–AcBDP [116, 117], referred to those of PM567.

The presence of *tert*–butyl groups at 1– and 6–positions (*t*Bu–AcBDP), instead ethyl groups (Et–AcBDP), increases the absorption (ε and f) and fluorescence (k_{fl}) transition probability, while the spectral bands position and the k_{nr} constant remain practically unaltered. The former effects could be ascribed to the inductive effect of the alkyl group which is higher in the *tert*–butyl substituent. However, the fact that the *tert*–butyl groups at 1– and 6–position does not noticeably affect the internal conversion of BODIPYs contrast with previous results in alkyl–BODIPYs discussed in Section 2.1, in the sense that *tert*–butyl groups at 1– and 7–position increase the internal conversion of PM597 due to a loss in the planarity of the chro-mophoric ring [87]. In the present case such effect disappears because the absence of substitu-ent at the adjacent 8 position facilities the accommodation of the *tert*–butyl group at the 1–position, unaltering the planarity of the pyrrole rings. For this reason, the *t*Bu–AcBDP de-rivative presents higher fluorescence capacity, with $\phi \approx 0.8$ and $\tau \approx 6$ ns values, with respect to the parent PM597 dye (Table 1) [117].

The solvatochromic shifts in the absorption and fluorescence spectra of these 3–acetamido–BODIPYs are similar to those observed for alkyl–BODIPYs. However, the ϕ value of the 3–acetamido derivatives is practically independent of the solvent characteristics, which contrasts with the highest ϕ values observed in polar/protic solvents for alkyl–BODIPYs. Moreover, 3–acetamido BODIPYs presents a new absorption band at higher energies (around 470 nm) in very acid ($[H^+] > 8\times10^{-2}$ M) ethanolic solution, with a decrease in the ϕ value from 0.70 to 0.36 but remaining the τ values practically constant. This decrease in the fluorescence efficiency is more pronounced after excitation at the new hypsochromic absorption band (ϕ = 0.15). These results suggest the formation of a new entity related to the protonation of the 3–acetamido–BODIPY dye in very acid media. The protonated species absorbs at shorter wavelengths and is not fluorescence (the shape of the fluorescence band is independent of the $[H^+]$), and induces a static quenching in very acid media [117]. Probably, such a protonation lead to a chemical reaction resulting in the loss of the BF_2 bridge. This fact will be discussed in Section 5.1 for a similar amino derivative. In any case, BODIPY dyes are chemically unstable in high acidity media [118].

3. Intramolecular Energy Transfer Processes : Multichromophoric BODIPY systems : In order to reach for new photophysical phenomena in BODIPY dyes, multichromophoric systems based on the incorporation of poly–*p*–phenylene moieties (biphenyl or terphenyl) at the 8 position of the PM567 chromophore (Scheme 3) are analysed in the present Section. Additionally, a multichromophoric di–BODIPY system, consisting in two PM567 cores linked by a terphenyl group at their *meso* positions (P3ArP, Scheme 3) is also considered [119, 120].

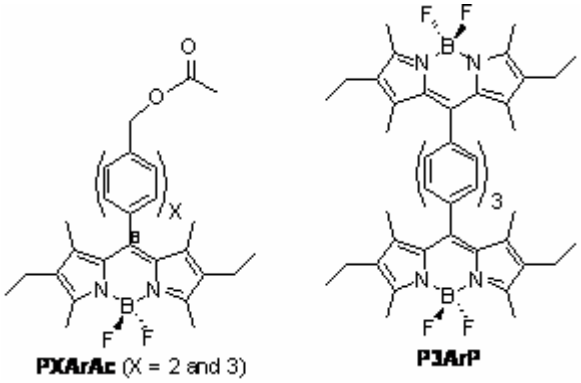

Scheme (3) : Chemical structure of multichromophoric polyphenylene−BODIPY dyes [119].

The UV–Vis absorption spectrum of these multichromophoric systems is composed of several absorption bands (Figure 8). The lowest energy absorption band is the typical $S_0 \rightarrow S_1$ electronic transition of the PM567 core. However, a new broad and structureless absorption band, non–observed in PM567, appears in the UV, which is attributed to the poly–*p*–phenylene moiety (Figure 8A). The same holds true for the trichromophoric dye P3ArP (Figure 8A, curve c), suggesting the absence of any intramolecular dimer state between the two BODIPY units. Probably the length and rigidity of the terphenyl linking group place far away both BODIPY rings, avoiding any overlap between the electronic π–systems of both BODIPY cores. The most remarkable feature of P3ArP is its high molar absorption coefficient ($\varepsilon_{max} \approx 1.5\times10^5$ $M^{-1}cm^{-1}$),

twice that of normal BODIPYs, indicating that the absorption transition of each BODIPY chromophore is additive. Indeed, quantum mechanical calculations reveal that the S_0–S_1 absorption band of P3ArP corresponds to promotion of an electron from the HOMO to the LUMO of each chromophore that means two independent electronic transitions [120].

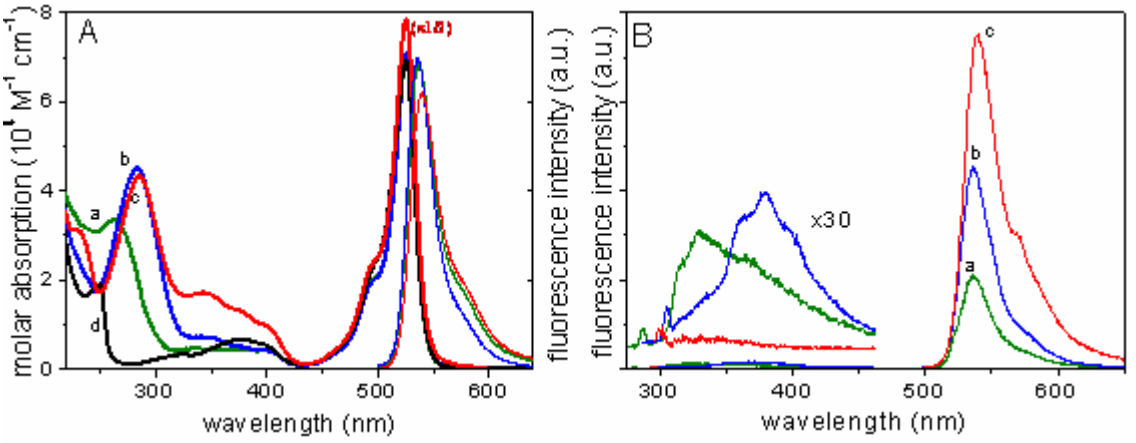

Figure (8) : (A) Absorption and fluorescence (under Vis excitation) spectra of P2ArAc (a), P3ArAc (b) and P3ArP (c) in c–hexane. The corresponding spectrum of PM567 (d) is also included for comparison. (B) Fluorescence spectra under UV excitation [119, 120].

The absorption spectra of these multichromophoric systems can be interpreted as the sum of the independent absorption bands of each chromophoric system, indicating the absence of any electronic coupling between the PM567 core and the 8–polyphenylene in the ground state. In fact, quantum mechanical calculations reveal that the first phenylene group (directly attached to the BODIPY core at the *meso* position) is disposed nearly perpendicular (dihedral angle 86.3º for P3ArAc) with respect to the PM567 ring. The theoretical simulation of the absorption characteristics of these multichromophoric dyes also suggests the presence of two main absorption bands: one located in the visible region (energy gap ΔE = 2.88 eV) with oscillator strength f = 0.41 corresponding to the S_0–S_1 transition of PM567; and another one placed in the UV region due to the first transition of the polyphenylene group: ΔE = 4.70 eV with f = 0.8 for P2ArAc, and ΔE = 4.30 eV with f = 0.9 for P3ArAc [120].

The excitation at the vibronic shoulder of the lowest energetic band (*ca* 490 nm) of PXArAc and P3ArP dyes leads to the typical intense Vis fluorescent band of PM567, being the mirror image of the corresponding absorption band (Figure 8A), with a low Stokes shift ($\Delta\nu_{St} \approx 550$ cm^{-1}). The photophysics of these dyes under Vis excitation remains quite similar to that of the PM567 analog with only one phenylene group at the 8–position (P1ArAc). Therefore, the number of phenylene units at the 8–position of the BODIPY core does not seem to strongly affect the photophysics of the chromophore.

On the other hand, the UV excitation leads to a weak fluorescence emission from the corresponding polyphenylene unit in the UV and to the typical strong Vis fluorescent band of the BODIPY group (Figure 8B). These results indicate the existence of an intramolecular excitation

energy transfer (intra–EET) process from the donor poly–*p*–phenylene to the acceptor BODIPY group. Consequently, the fluorescence emission of the poly–*p*–phenylene chromophore is strongly quenched ($\phi < 0.02$). This Vis emission is far away from the UV excitation, leading to a very large "*pseudo*" Stokes shift ($\Delta\nu_{St} \approx 17700$ cm^{-1}), one of the largest observed in BODIPY dyes. Dyes with large Stokes shifts are demanded for their use as fluorescence labels and probes, since scattering interferences of the pumping/excitation light are neglectable at the emission detection region. The intra–EET process is very efficient for the P3ArP dye, since the emission from the terphenyl unit is practically not observed, Figure (8B). This is attributed to the presence of two BODIPY acceptor units connected to the polyphenylene donor group.

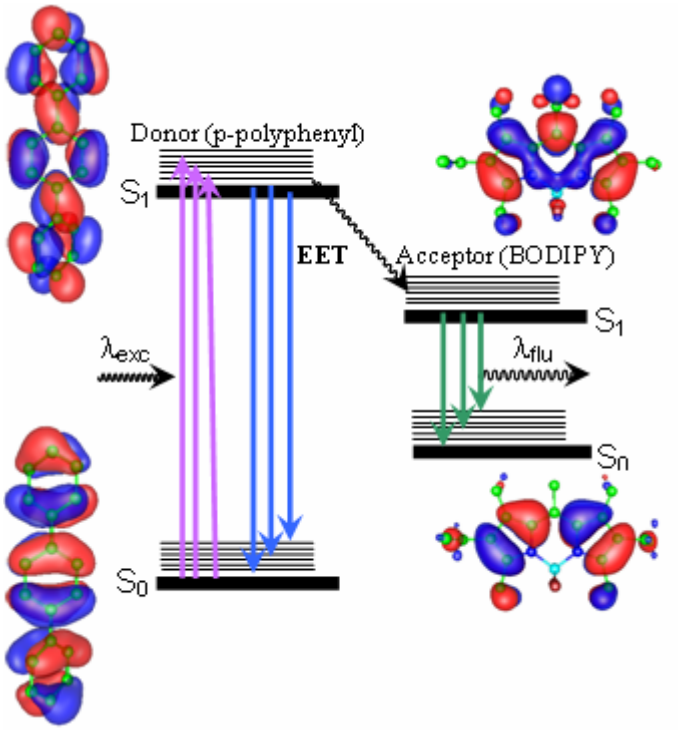

Scheme (4) : Intra-EET mechanisms in PXArAc and P3ArP dyes, together with the electronic density in the HOMO and LUMO states of PM567 and *p*terphenyl dyes [120].

In order to study the dynamics of the intra–EET, time–resolved fluorescence decay curves at different excitation and emission wavelengths were registered. The fluorescent decays of the free related chromophores, terphenyl and PM567, are well described by a monoexponential analysis, with lifetimes of around 1 ns and 6 ns, respectively. The fluorescent decay after direct excitation of the BODIPY ($\lambda_{exc} = 490$ nm) in the bichromophoric P3ArAc dye, was also monoexponential with $\tau = 4.8$ ns, lower than that of the parent PM567 dye. This decrease was also observed for the 8–phenyl–PM567 analog ($\tau = 5.0$ ns), ascribed to an enhancement in the non–radiative deactivation rate constant probably due to a vibrational coupling between both entities. However, the fluorescence decay after UV excitation of the *p*–terphenyl moiety in P3ArAc ($\lambda_{exc} = 275$ nm, $\lambda_{fl} = 370$ nm) becomes biexponential: a main component (98 %) with a short lifetime (< 1ns), lower than that of the free terphenyl unit; and a minor component (2 %)

with a longer lifetime (4.6 ns). The fluorescent Vis decay of the BODIPY component (λ_{fl} = 535 nm) after UV excitation (λ_{exc} = 275 nm) was analyzed by a grown–in component with a short lifetime (< 1ns) and a decay component with a fluorescence lifetime of 4.75 ns, suggesting that the maximum population of the fluorescent excited state is reached after a delay time after excitation. All these results confirm a fast intramolecular energy transfer (in the subnanosecond time–scale) from the excited state of the donor terphenyl to the acceptor BODIPY chromophore. Scheme 4 illustrates this intramolecular excitation energy transfer (intra–EET) process.

Different mechanisms can be used to explain this intra–EET process [121]. In the long–range dipole–dipole coupling mechanism proposed by Förster [122,123], the rate constant of the energy transfer depends mainly on the spectral overlapping between the fluorescence band of the donor moiety and the absorption band of the acceptor entity. Taking into account the low spectral overlap observed between the fluorescence of terphenyl group and the S_0–S_1 absorption band of PM567 (Figure 9), the long range mechanism can be considered as neglectable in the present P3ArAc case. Moreover, quantum mechanical calculations predict that the transition dipole moment is polarized along the longer molecular axis of each chromophore, leading to a perpendicular disposition of both dipoles in P3ArAc (Figure 9). This theoretical result confirms the absence of any significant Förster resonance energy transfer. On the other hand, the short–range exchange interaction EET mechanism proposed by Dexter [124] implies an overlap between the electronic clouds of the involved partners. This means that the corresponding rate constant for the present P3ArAc case should be very low, since the electronic π–systems of both moieties are disposed nearly perpendicular.

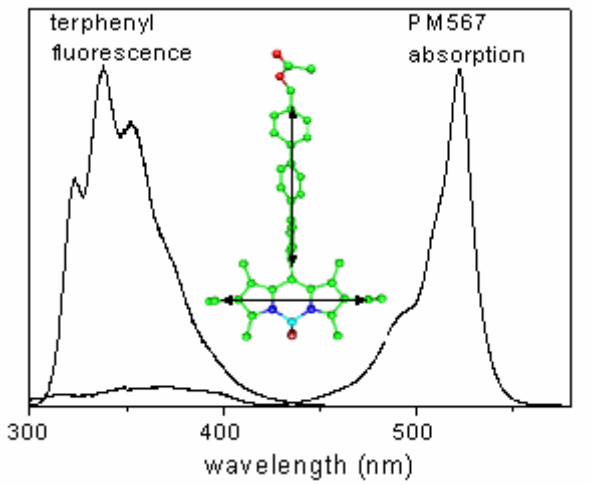

Figure (9) : Spectral overlap of the normalized absorption spectrum of PM567 and fluorescence band of terphenyl group. Inset: mutual orientation of the transition moments of each dye in P3ArAc [120].

An alternative mechanism for the intra–EET process consists on the energy transfer between the donor to the acceptor through the chemical bond linking both moieties [125 – 128]. This mechanism demands an orbital interaction between both entities. The corresponding HOMO and LUMO contour maps of terphenyl and PM567, illustrated in Scheme (4), indicate that exist an important orbital interaction in the LUMO state between both chromophores through the

linking 8–position of BODIPY core. This observation supports the validity of the through–bond mechanism for the intra–EET in the terphenyl–PM567 system, similar to that proposed for other anthracene–BODIPY or porphyrin–BODIPY systems [129 – 132]. In any case, small contributions of the long–distance EET Föster mechanism cannot be excluded because of the weak overlapping between the fluorescence band of the terphenyl group and the S_0–S_2 absorption band of the BODIPY chromophore, as has been proposed for several 8–pyrenyl substituted BODIPYs [133 – 137].

4. Charge Transfer Excited States : Cyano-BODIPY dyes :

As has been discussed above, the presence of electron donor or acceptor substituents can modulate the emission region of BODIPYs. However, the presence of electron rich functional groups can in some cases induces the appearance of new photophysical phenomena, which usually are sensitive to the solvent properties or the presence of certain molecules in the surrounding media. These processes span the commercial and technological applicability of BODIPY dyes in other fields, apart from their inherent use as the active media of tunable lasers.

The absorption and fluorescence bands of the commercial PM650, with a cyano group at the *meso* 8–position [138] are collected in Figure (10). This dye absorbs ($\lambda_{ab} \approx 590$ nm) and emits ($\lambda_{fl} \approx 600$ nm) in the red region, with an important bathochromical shift of around 60 – 65 nm with respect to PM567. Besides, the presence of the cyano group reduces the intensity of both bands, mainly in polar/protic solvents (Figure 10).

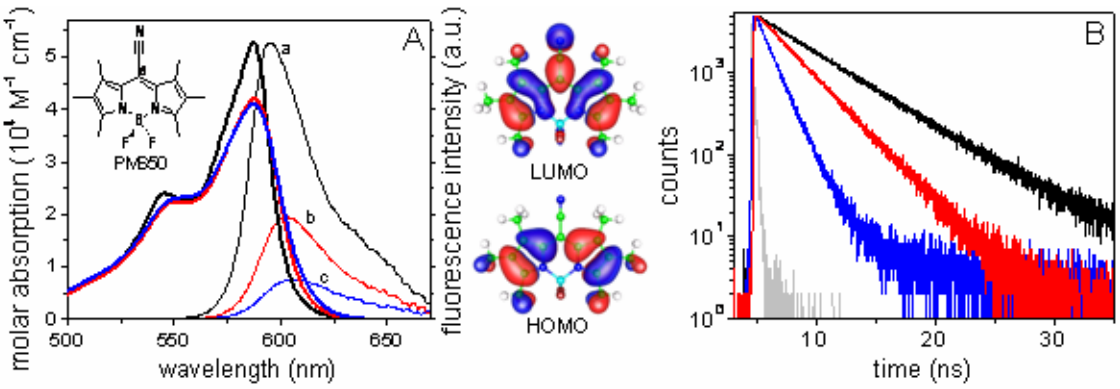

Figure (10) : (A) Absorption and fluorescence of PM650 in diluted solutions of c–hexane (a), dioxane (b) and methanol (c). (B) Fluorescence decay curves of the dye in those solvents. The contour maps of the HOMO and LUMO state are also included [138].

Table (3) summarizes the photophysical properties of PM650 in a multitude of solvents with different physicochemical properties [138]. The observed large solvatochromic shift to lower energy by increasing the solvent polarity is also predicted by theoretical calculations. Such bathochromic shift can be interpreted by means of the contour maps of the HOMO and LUMO states shown in Figure (10). The presence of the strong electron withdrawing cyano group at central position of the chromophoric core implies a net stabilization of the LUMO level, characterized by a much higher electronic density at this 8–position, than the HOMO state. Consequently, the energy gap between the HOMO and LUMO states decreases, leading to the ob-

served red shift of the spectral bands. On the other hand, the electron removal inductive effect of the cyano group reduces the delocalisation of the π–system of the chromophore, leading to a decrease in the k_{fl} value, which correlates with a diminution of the absorption intensity (analyzed by the molar absorption coefficient ε_{max}), as is shown in Table (3).

Table (3) : Photophysical properties of PM650 (2×10^{-6} M) in a wide variety of solvents [138]

Solvent	λ_{ab} (nm)	ε_{max} (10^4 M^{-1} cm^{-1})	λ_{fl} (nm)	ϕ	τ (ns)
1. 2–methylbutane	586.6	5.28	596.0	0.45	5.23
2. n–hexane	587.6	5.20	597.2	0.44	5.14
3. c–hexane	589.3	5.30	599.6	0.36	4.67
4. isooctane	587.5	5.28	597.2	0.41	4.86
5. diethyl ether	587.4	3.65	601.6	0.30	3.44
6. 1,4–dioxane	589.8	4.25	607.2	0.19	2.89
7. THF	590.0	2.93	606.4	0.18	2.46
8. acetona	587.9	3.45	606.0	0.11	1.81
9. Methyl formate	587.6	4.25	605.2	0.15	2.17
10. Methyl acetate	587.8	4.25	604.8	0.16	2.38
11. Ethyl acetate	587.8	4.17	603.2	0.15	2.37
12. Buthyl acetate	588.9	4.48	603.6	0.19	2.71
13. Acetonitrile	588.0	2.85	605.6	0.096	1.73
14. 1–octanol	591.1	4.37	605.6	0.17	2.58
15. 1–hexanol	590.5	4.29	607.6	0.14	2.31
16. 1–butanol	590.0	4.17	607.6	0.13	2.02
17. 1–propanol	589.6	4.00	606.8	0.13	1.83
18. Ethanol	588.7	4.05	608.0	0.099	1.64
19. Methanol	587.5	4.10	609.2	0.060	1.29
20. F3–ethanol	589.9	3.80	614.4	0.040	1.14

The absorption band position of PM650 hardly changes with the solvent whereas the fluorescence band shifts bathochromically in polar/protic solvents, leading to a moderate increase of the Stokes shift. This evolution is opposite to the typical hypsochromic shift observed for alkyl–BODIPYs in polar media (Table 2). The corresponding multilinear analysis of the fluorescence wavenumber and Stokes shift with different solvent parameters provide good linear relationship (correlation coefficient, $r > 0.95$), as can be observed in Figure (11). The adjusted coefficients suggest that the evolution of these spectroscopic parameters with the solvent characteristics are mainly due to the solvent polarity (relatively-high c_{π^*} values, inset Figure 11), being minor the effect of the solvent acidity (moderate c_α values) and practically negligible the solvent basicity (low or null c_β values). Therefore, an increase of the solvent polarity and acidity leads to a diminution and augmentation of the fluorescence wavenumber and Stokes shift, respectively. Indeed, quantum mechanics results indicate that the dipole moment of the PM650 slightly increases upon excitation, the opposite evolution to that obtained for alkyl–BODIPY dyes above discussed [138].

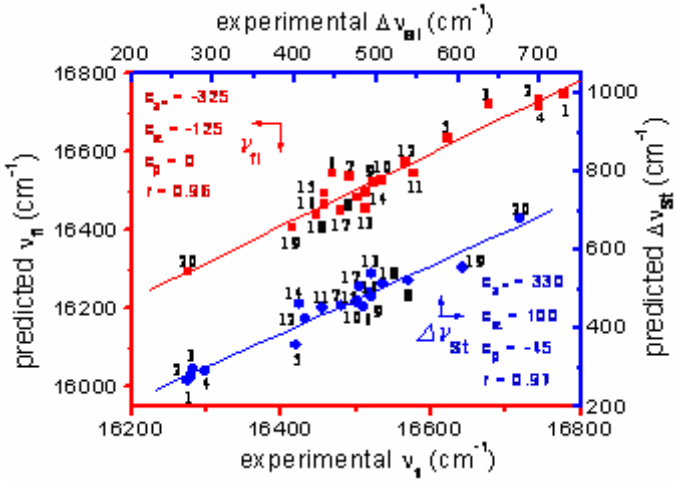

Figure (11) : Multiple linear regression of the fluorescence wavenumber and Stokes shift of PM650 in a wide variety of solvents using the Taft solvent scales (from apolar 1 to polar/protic 20, see Table 3) [138].

Moreover, the ϕ and τ values of PM650 drastically decrease in polar/protic solvents due to both a diminution in k_{fl} value and, mainly, to an important increase in k_{nr}. These behaviours contrast with those reported for alkyl–BODIPY dyes (see Section 2.2) [27, 32]. The slight decrease of the k_{fl} values in polar solvents can be assigned to the electron removing effect of the cyano group, which is favoured in polar solvents. On the other hand, the solvent effect on the k_{nr} of PM650 is analyzed by a multilinear relationship in Figure (12). The k_{nr} value (k_{nr} values in Figure 12 are represented in the natural logarithm scale) strongly increases with the solvent polarity/polarizability ($c_{\pi^*} = 4.1$, much higher than c_α and c_β). Quantum mechanical calculation reveals a planar π–system in the excited state, preventing any internal conversion mechanism related to the flexibility of the BODIPY chromophore. Consequently, an extra radiationless deactivation via the formation of a non–fluorescent intramolecular charge transfer (ICT) state, obtained after the transfer of an electron from the excited state of the BODIPY core to the cyano group, has been proposed [139]. The mechanism for the formation of this ICT excited

state is illustrated in Scheme (5). The imminent effect in the formation of this photoinduced ICT state is a fluorescence quenching process for the emission from the locally excited state of the BODIPY chromophore. This ICT state would be characterized by a high dipole moment, and hence would be stabilized in polar media, quenching the LE emission more efficiently in such solvents.

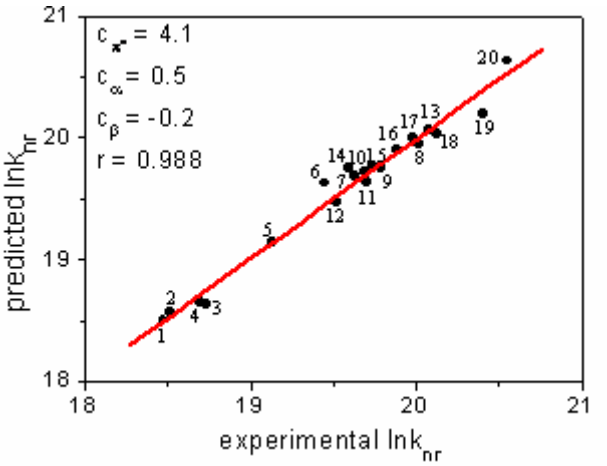

Figure (12) : Correlation between the experimental and predicted (by means of the Taft solvent scales) values of non–radiative rate constant k_{nr} of PM650 in many solvents (from apolar 1 to polar/protic 20, see Table 3) [138]. Data are expressed in natural logarithm scale.

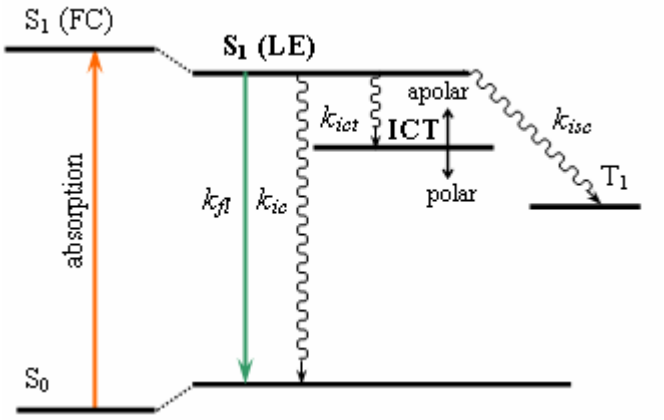

Scheme (5) : Energy diagram for the deactivation processes from the S_1 excited state of PM650: LE (Localize Excited), FC (Franck–Condon) and ICT (Intramolecular Charge Transfer) states. Continuous and dotted lines represent radiative and non–radiative processes, respectively [138].

The strong dependence of the fluorescence properties of PM650 with the solvent polarity suggests the possibility of use this BODIPY dye as a fluorescent molecular probe in the characterization of the polarity of the surrounding environment [138].

On the other hand, it has experimentally observed that the colour of PM650 in certain solvents can change after sample preparation [140]. Thus, in some N,N'–dialkyl amides (*i. e.*

N,N'–dimethyl formamide, DMF), the colour of the PM650 solution changes from violet, the normal tonality of PM650 dye, to green just during sample preparation. These solvents are characterized by their high polar and basic characters [91] (for instance, $\pi^* = 0.88$ and $\beta = 0.69$ for DMF). In other N–alkyl or non–alkyl amides (N–methylformamide, MF and formamide, F), the change of the colour takes place in a few days after sample preparation. With respect to DMF, these last solvents are more acid (*i.e.* $\alpha = 0.71$ for F *vs* $\alpha = 0$ for DMF) [91]. In other non–amide solvents with high electron donor ability (such as 2–pentanona and diethyl ether), the samples became nearly transparent after several days. In apolar (c–hexane), low–basic (di-oxane) and polar/protic (methanol) solvents, the colour of PM650 remains unaltered for several weeks. Such effects have never been reported before in any BODIPY dye and are related with the presence of the cyano group [140].

Figure (13) compares the absorption and fluorescence spectra of freshly prepared PM650 solutions in DMF and in acetone, two solvents with similar polarity and basicity but different acidity. The absorption and fluorescence bands of PM650 in DMF are drastically shifted to higher energies (100 nm in absorption and 70 nm in fluorescence) with respect to those in acetone, leading to an important Stokes shift (up to 2000 cm^{-1}). Surprisingly, while the absorption probability of PM650 decreases in DMF, the fluorescence capacity significantly increases ($\phi = 0.40$ and $\tau = 5.15$ ns) with respect to that in acetone ($\phi = 0.11$ and $\tau = 1.81$ ns). These results suggest that the ICT excited state of PM650 in polar solvents is not longer formed in this amide solvent. Moreover, the hypsochromic absorption and fluorescence bands of PM650 in amide media tend to disappear after ageing the samples during several weeks [140].

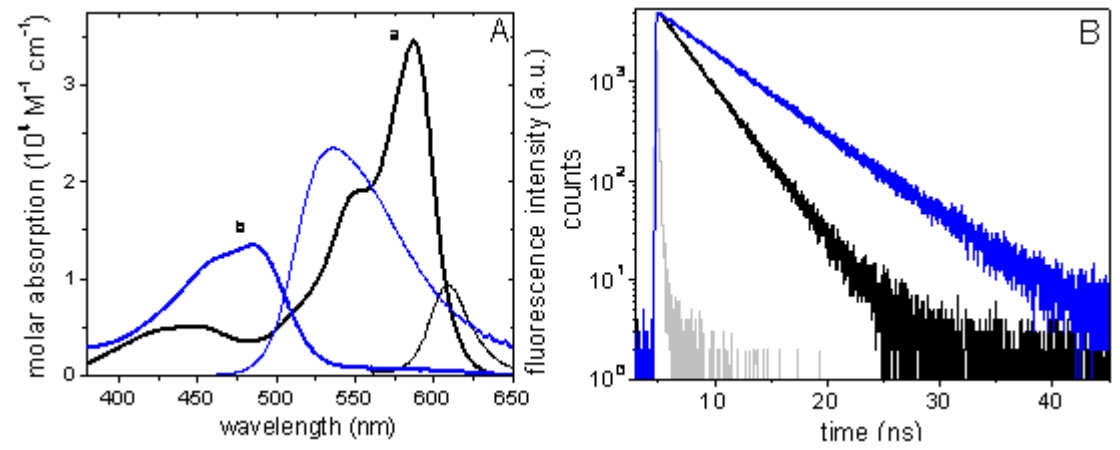

Figure (13) : A) Absorption and fluorescence (scales by their ϕ value) and B) fluorescence decay curves of PM650 in acetone (a) and DMF (b) [140].

To get a deeper understanding of the change in the color and posterior degradation of PM650 dye in amides, the photophysical properties of the dye were registered at several ageing times in DMF/dioxane mixtures. Dioxane was chosen as an "inert" solvent, since the photophysical properties of this dye do not depend on the ageing. For a low DMF content mixture (16 %), the absorption spectrum for not ageing sample (t = 0), measurements just after sample preparation, present the typical absorption band of PM650, centered at around 590 nm (Figure 14(left)). The

ageing of this sample induces the presence of a new absorption band at lower energies of the main absorption band. The absorbance of the 590 nm absorption band decreases and those at 460 and 490 nm slightly increases with the ageing time.

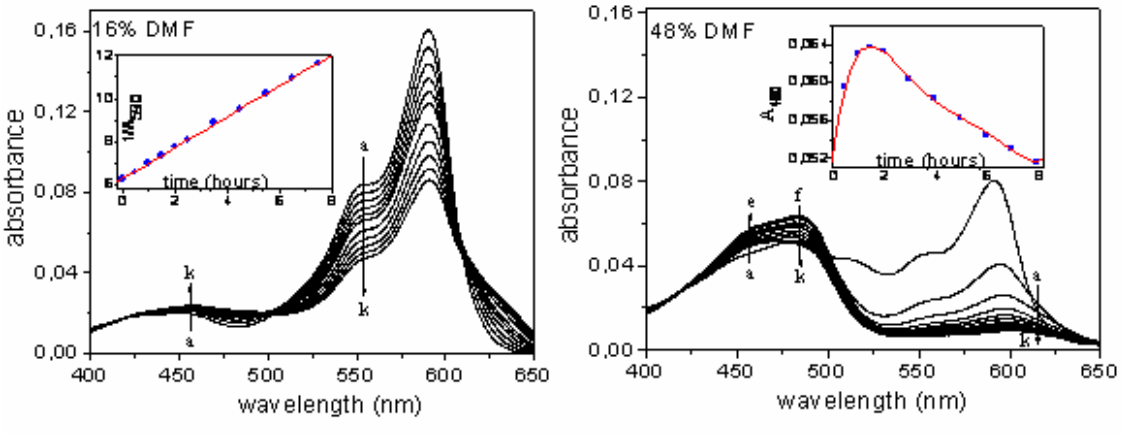

Figure (14) :Evolution of the absorption spectra with the ageing time, from 0 (a) to 8 hours (k), of PM650 in DMF/dioxane mixtures (left 16 % and rigth 48 % in DMF) [140]. Inset shows evolution of the absorbance at specific absorption wavelengths with the ageing time.

On the other hand, for a moderate DMF content DMF/dioxane mixture of 48% and freshly prepared sample, the intensity of the typical green/red absorption band of PM650 at 590 nm is drastically reduced whereas those blue bands at 460 and 490 nm become important (Figure 14(right)). The red/green absorption band diminishes with the ageing time, and becomes practically undetected after 8 hour of the sample preparation. The blue absorption bands firstly increases their intensities with the ageing time up to maximum value at around 90 minutes after the sample preparation from which their intensities decrease with the ageing.

The loss in the typical green/red absorption band of PM650 ($\lambda_{ab} \approx 590$ nm) with the aging and the DMF content is an irreversible process and could be ascribed to a chemical reaction between PM650 (via the cyano group) and DMF molecules [140]. HPLC analysis indicates the appearance of several products of PM650 in pure DMF. The main one should be the responsible for the new blue absorption bands at 460 and 490 nm. ^{1}H–NMR data of this compound seem to indicate the replacement of the methyl groups at 2– and 6–positions by H–atoms, with a non–hydrogen substituent at the 8–position. Therefore the cyano group is not exchanged by a proton but probably it is reconverted into a carboxylic group (likely by an oxidation process). A second minority compound could be related with the loss of the CN group from the aromatic π–system of the PM650 core. Quantum mechanics calculations at the TD–B3LYP level confirm that both chemical structures would lead to a hypsochromic shift of the S_0–S_1 transition [140].

The kinetics of the chemical reaction between PM650 and DMF are analyzed from the time–evolution of the disappearance and appearance of the green/red ($\lambda_{ab} \approx 590$ nm) and the blue ($\lambda_{ab} \approx 480$ nm) absorption bands, respectively, observed for PM650 in DMF/dioxane mixtures. The corresponding evolutions of the absorbance of these bands with the ageing time are

inset in Figure (14). For a 16 % DMF content, the disappearance of PM650 follows a pseudo–second order kinetic with respect to PM650 ($1/A_{590}$ *vs* t, r = 0.9998, inset Figure 14(left)). For higher DMF content (*i.e*. 48%), the kinetic order for the loss of the 590 nm absorption band is not so clear. For such a mixture, the time evolution of the absorbance at 480 mm (inset Figure 14(right)) confirms the presence of two consecutive mechanisms for the PM650 degradation in electron donor solvents: a first process involved with the formation of a PM650–DMF complex (probably due to solute–solvent interaction through the cyano group); and a second slower process related with the owing bleaching of the dye. This degradation phenomenon is not an oxidation process, since it was observed to take also place in an inert atmosphere of N_2 [140].

The formation of the PM650–DMF complex is characterized by an activation energy, which can be evaluated from the evolution of the interchange of the 590 and 460 nm absorption bands with the temperature. An energy barrier of ~ 3 kcal mol^{-1} was reported for the present system [140].

5. Proton Sensor BODIPY Dyes :

5.1 Charge Transfer Complex : Amino BODIPY Derivative :

As has been discussed above, the incorporation of an electron withdrawing cyano group at *meso* position of the chromophore leads to the important changes in the photophysical properties of the BODIPY chromophore, which becomes highly sensitive to the environmental properties. In view of such trends, the photophysical properties of a BODIPY derivative bearing an electron donor amino group directly linked to the 3 position of the BODIPY core, the so–called Am–BDP (scheme inset Figure 15), were also evaluated [116, 117]. The absorption and fluorescence bands of this derivative in three representative solvents are shown in Figure (15) and its photophysical properties are summarized in Table (4).

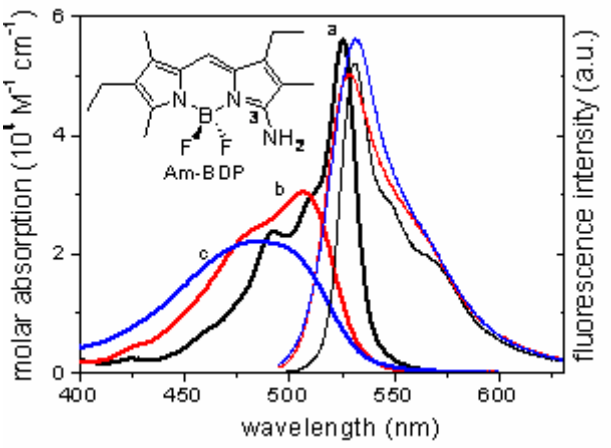

Figure (15) : Absorption and fluorescence spectra of 3–amino BODIPY (Am–BDP) in diluted solutions of c–hexane (a), ethyl acetate (b) and trifluoroethanol (c) [116, 117].

The photophysical parameters of Am–BDP in apolar solvents are similar to those of alkyl–BODIPYs, although the fluorescence quantum yield is nearly insensitive to the solvent characteristics. However, the shape of the absorption band of Am–BDP changes in polar/protic media (Figure 15), from a vibrational structured absorption band obtained in apolar environments to a broader and less intense and hypsochromically shifted absorption band in polar media. The total absorbance (area under the absorption band) is, however, nearly solvent independent (f value in Table 4). On the other hand, the fluorescence band remains that of other BODIPY dyes, in spite of changing the characteristics of the media (Figure 15), but with a larger Stokes shift (1150 cm^{-1}) in polar/protic solvents owing to the hypsochromic shift of the absorption bands.

Table (4) :Photophysical properties of 3–amino-BODIPY (2×10^{-6} M) in six representative solvents [116, 117]

Solvent	λ_{ab} (nm)	ε_{max} (f) (10^4 M^{-1} cm^{-1})	λ_{fl} (nm)	ϕ	τ (ns)
c–hexane	525.6	5.6 (0.37)	532.4	0.64	4.06
ethyl acetate	506.4	3.0 (0.36)	529.2	0.62	3.89
acetone	502.4	3.0 (0.38)	529.8	0.62	4.01
methanol	498.8	2.7 (0.39)	529.0	0.64	4.21
ethanol	503.2	2.8 (0.37)	529.4	0.65	4.17
F3–ethanol	~ 485	2.2 (0.36)	531.9	0.69	5.20

Taking into account the electron donor character of the amino substituent, one could expect the formation of an intramolecular charge transfer (ICT) complex between the BODIPY unit and the amino group. This charge transfer complex should be stabilized in polar environments and would already exist in the ground state, because the spectral changes are observed in the absorption band. The ICT complex should be non fluorescent, since the shape of the fluorescence band is solvent independent (Figure 15).

Because the electron donor capacity of the amino group would be strongly affected by the protonation of its electron lone–pair, the photophysics of Am–BDP derivative is pH dependent [117]. Figure 16 shows the evolution of the absorption and fluorescence spectra as a function of the H^+ and OH^- concentrations in ethanol. The absorption intensity progressively decreases from basic media to moderately acidifying the solvent, without any appreciable change in the shape of the absorption band (from curve a to curve e in Figure 16). But in solutions with $[H^+]$ in the range 3×10^{-8}–4×10^{-4} M (from curves f to g, Figure 16), the absorbance at the vibronic shoulder increases in detriment of the main absorption band, and at $[H^+] > 2\times10^{-3}$ M a new hypsochromic band appears at $\lambda_{ab} \approx 460$ nm (from curves h to l in Figure 16). These changes correlate with the modifications observed in the shape of the absorption band of Am–BDP in trifluoroethanol (Figure 15), a high–acid solvent. The excitation at this new absorption band

induces a drastically decrease in the fluorescence intensity ($\phi < 0.1$) and the emission band becomes broader, (Figure 16). The fluorescence decay curves cannot be further analyzed as monoexponentials but rather as multiexponential.

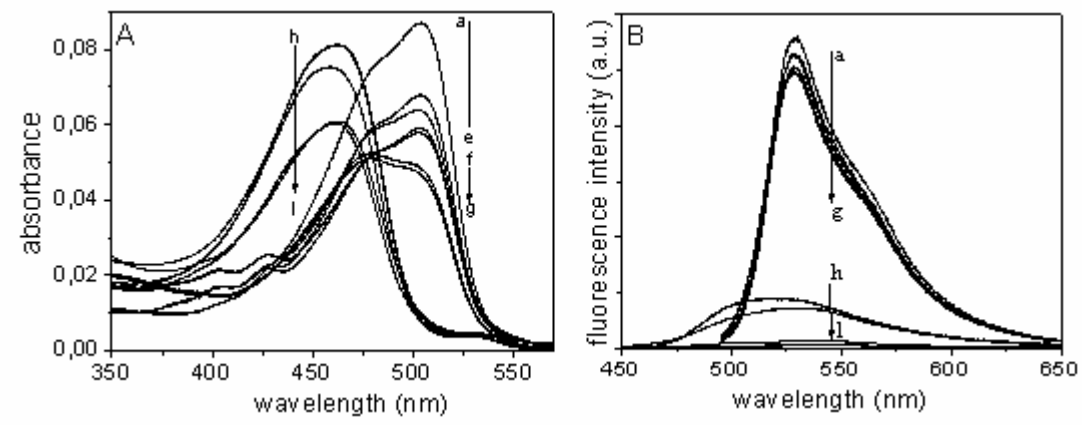

Figure (16) : Absorption (A) and fluorescence (B) spectra of 3–amino BODIPY in acid and basic ethanolic solutions [117] (from $[OH^-] = 3\times10^{-3}$ M (a) to $[H^+] = 3\times10^{-6}$ M (e), from $[H^+] = 4\times10^{-5}$ M (f) to $[H^+] = 4\times10^{-4}$ M (g) and from $[H^+] = 2\times10^{-3}$ M (h) to $[H^+]= 8\times10^{-2}$ M (l)).

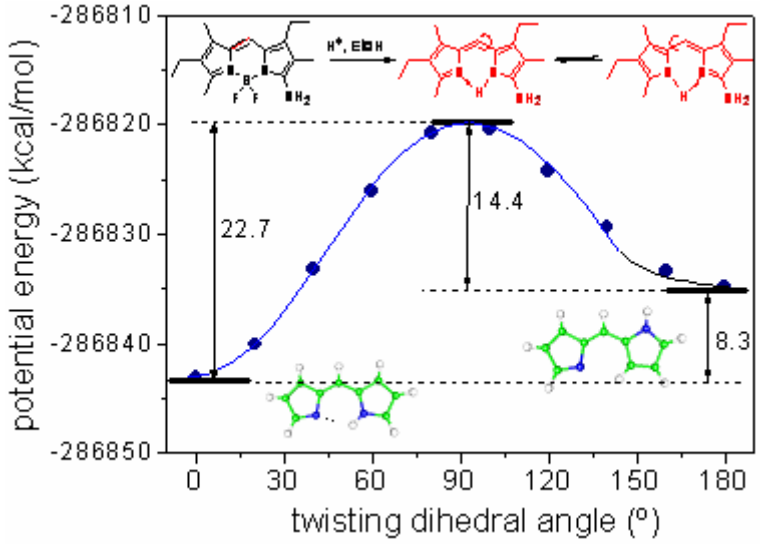

Figure (17) : Conformational potential energy curve of BODIPY core calculated by the B3LYP method. Inset, scheme of the loss of BF_2 group in acid media [117].

This effect of the solvent acidity on the photophysics of amino–BODIPY is not a general reversible acid–base equilibrium, since a cyclic external modification in the pH does not correspond with the expected evolution in the absorption and fluorescence spectra. Moreover, the appearance of the hypsochromic absorption band in acid solutions, immediately after sample preparation, is also observed in aged solutions with moderate $[H^+]$ concentrations. These results

suggest the formation of a degradation product of the amino–BODIPY in acid media. HPLC measurements indicate that in such conditions, the dye loss the BF_2 unit, as it is shown in the scheme inset of Figure (17). This process should take place via the protonation of the NH_2 group [117].

The break of the BF_2 bridge disrupts the chromophoric π–system, leading to a decrease of the aromaticity of the system and to a new hypsochromic absorption band. Now, the two pyrrole units could rotate in the excited state around the methylene linking group, decreasing drastically the fluorescent ability of the dye. Moreover, proton transference between both N atoms of the pyrrole units in the excited state cannot be discarded, giving rise to an extra non–radiative loss of the excitation energy. In addition, the NH_2 substituent could also acts as a proton donor group, increasing in this way the intramolecular proton transfer probability. All these phenomena can explain the poor fluorescent ability of amino–BODIPY in acid media.

The conformational flexibility of the compound resulting of the loss of the BF_2 unit is theoretically confirmed by means of the potential energy curve (Figure 17) around the connecting single bond between both pyrroles. The most stable conformation has the two pirrole units coplanar (*Z–syn* form, dihedral angle 0º), likely stabilized by an NH...N intramolecular H–bond. The *Z−anti* conformation (dihedral angle 180º), where this bond cannot be formed, must be a less stable state (Figure 17). The energy barrier for the change *Z–syn*→*Z–anti* transition is 22.7 kcal mol^{-1}. This relatively high−energy barrier should be a consequence of the single/double bond character of the methene bridge group linking the two pyrrole moieties, owing to the two extreme tautomeric structures of this system (Figure 17) [141, 142]. These results suggest the important role of the BF_2 bridge to achieve a rigid structure and, hence, highly fluorescent ability for BODIPY dyes.

5.2 Photoinduced Electron Transfer Processes in BODIPYs :

The bichromophoric dye P2ArOH, which structure is depicted inset Figure (18), consists in the PM567 dye bearing at its *meso* position the *p*–phenylphenol chromophore.

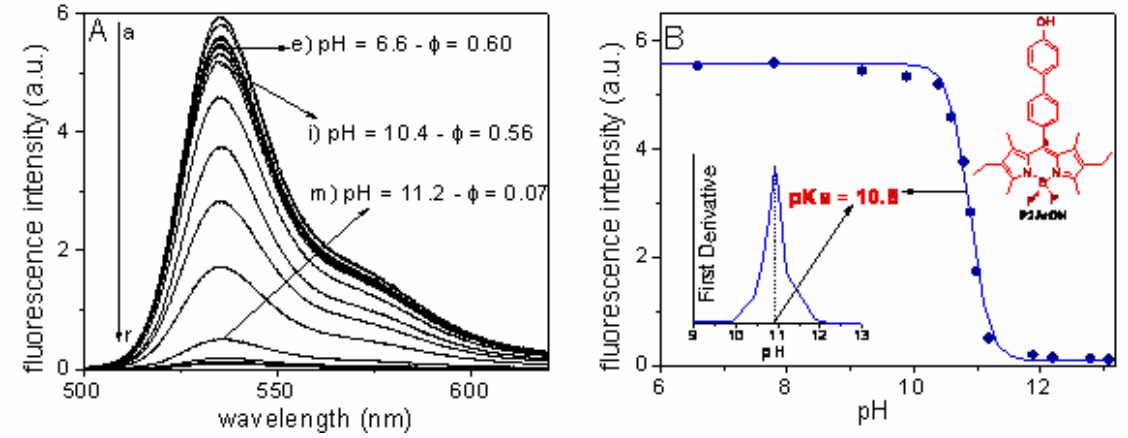

Figure (18) : Fluorescence spectra evolution of P2ArOH with the solvent basicity in ethanol [120] (from pH = 0 (a) to pH = 13.1 (r)).

Its photophysical properties under visible excitation are very similar to those of its partner P2ArAc (Scheme 3), and also shows the above discussed intra–EET process under UV excitation to reach the Vis emission (Section 3) [120]. However, both dyes differ in their photophysical behaviour in acid/basic media, because the properties of P2ArOH strongly depend on the ionization of its phenol group.

The absorption spectrum of P2ArOH in ethanol remains nearly independent of the pH of the media in the 0–13 pH range. However, the Vis fluorescence band drastically decreases in basic media, as is shown in Figure 18. The fluorescence quantum yield slight decreases from $\phi = 0.60$ in very acid media ($[H^+] = 1$ M) to 0.56 at moderate basic media (pH = 9.2). Further pH increase implies a strong decrease in the fluorescence quantum yield, reaching a ϕ value < 0.07 at pH = 13.1 (Figure 18A). The proton association constant (K_a) obtained from the evolution of the fluorescence intensity with the pH is 1.6×10^{-11} (Figure 18B). This value is quite similar to that reported for *p*–phenylphenol ($K_a = 1.4\times10^{-11}$ in water/ethanol mixture) [143].

The decay curves of P2ArOH are well analyzed as monoexponentials with $\tau = 5.05$ ns in the pH range 0–10.8. In more basic environments the fluorescent decay becomes biexponential, with a major component (98 %) with a lifetime of 4.8 ns, and a minor one (2 %) with a shorter lifetime (0.7 ns). Moreover, the fluorescence quenching in basic media is reversible, since the bright emission of the BODIPY group is recovered after sample acidification. These results suggest that P2ArOH can be applied as a reversible fluorescent sensor for acid/base media.

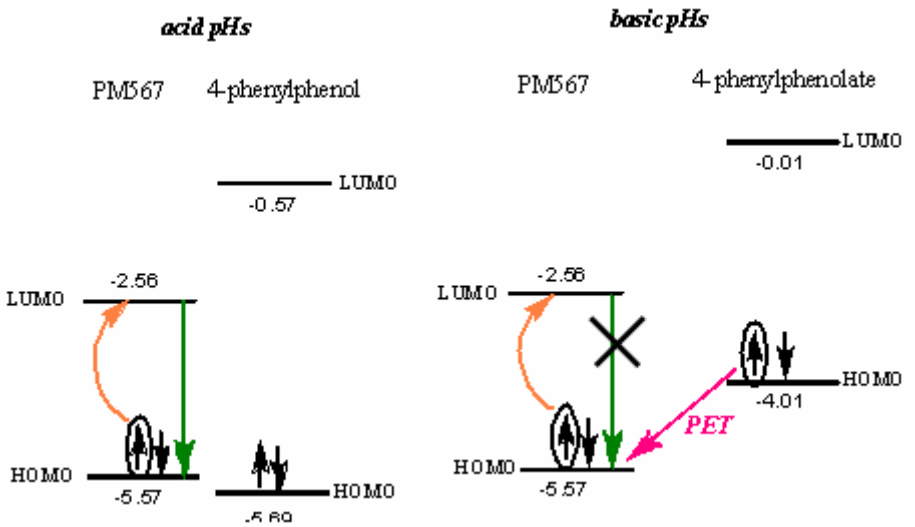

Scheme (6) : Calculated energy (in eV) of the frontier orbitals of PM567 and 4–phenylphenol in its neutral (acid pHs) and ionized (basic) forms in ethanol [120].

The experimental results can be interpreted on the basis of quantum mechanical calculations. The theoretical energy levels for the frontier HOMO and LUMO orbitals of PM567 and *p*–phenylphenol in ethanol, in its neutral and ionized forms, are illustrated in Scheme (6). In acid media (neutral form), the HOMO and LUMO orbitals of *p*–phenylphenol are placed at lower and higher energies, respectively, with respect to the corresponding HOMO and LUMO

states of the BODIPY chromophore (Scheme 6, left). However, in highly basic media the OH group is ionized and the energy of the frontier orbitals of the resulting *p*–phenylphenolate increases in such a way that its HOMO orbital is placed between the HOMO and LUMO levels of the BODIPY chromophore (Scheme 6, right). Consequently, when the BODIPY core is excited, an electron from the HOMO state of the ionized phenol can be spontaneously transferred (at least, the process is thermodynamically favored) to the HOMO state of the BODIPY, filling the semivacant HOMO orbital and avoiding the radiative transition of the excited electron back to the ground state [120]. Therefore, the loss in the fluorescent ability of P2ArOH in basic media could be assigned to a photoinduced electron transfer (PET) process [3 – 5] from the HOMO state of the ionized phenol group to the semivacant HOMO state of excited BODIPY core.

Consequently, P2ArOH can be considered as a versatile fluorescent dye. It shows a large Stokes shift under UV excitation at the phenylphenol group, giving rise to the BODIPY bright fluorescent emission via an efficient intra–EET process. Besides, this dye can also be used as a switch on/off proton sensor due to the reversible dependence of its fluorescence emission with the acidity/basicity of the medium by means of the deactivation/activation of a fluorescence quenching PET process.

6. Conclusions :

BODIPY dyes are characterized by a versatile organic chromophoric system. Their spectroscopic and photophysical properties have their important applications in photonic, as the active media in syntonizable dye lasers. Probably BODIPY dyes are becoming the most used laser dyes in the green/red Vis spectral region [144]. The incorporation of adequate substitution patterns allows the covalent linkage of the BODIPY chromophoric system to polymeric chain, an adequate strategy to develop tunable dye lasers in the solid state. Indeed, solid polymeric host materials not only ameliorate the photophysical properties of the BODIPY dye but also considerably enhance the photo and thermal stability of BODIPYs, increasing the operative lifetime of the photoactive system.

The design of new molecular structures based on the BODIPY chromophore with specific photophysical properties is essential for the application of these dyes in other fields such as fluorescent probes, antenna systems, etc. The presence of functional groups in the molecular structure of the BODIPY allows the modulation of the emission region of BODIPYs. An extension of the π–system through styryl groups at the 3– and/or 5–position or the presence of electron acceptor (cyano) or donor (acetamido) groups at the *meso* 8–position or 3–position, respectively, shifts the emission signal to the red, a very interesting spectral region from a technological point of view. Besides, the presence of such electron donor/acceptor groups gives rise to new photophysical phenomena sensitive to the solvent properties. Thus, these BODIPYs can be used as fluorescent probes to monitoring the characteristics of the surrounding environments of the dye. In this sense, the presence of a cyano group at the 8−position induces the formation of a non−fluorescence intramolecular charge transfer state, which quenches the fluorescence emission in polar solvents. Besides, this group chemically reacts with electron donor solvents appearing new hypsochromic absorption bands. Thus, PM650 dye can act as a sensor of polarity and electron donor capacity of the environment in the red part of the visible region. On the other hand, the incorporation of an amino substituent at the central *meso* position of the

BODIPY core leads to a chemical reaction in protic media providing a non–fluorescence derivative. Consequently, this dye can be used to monitor the environmental acidity. Moreover, the presence of a phenol group at the 8–position induces the appearance of a reversible quenching process via a photoinduced electron transfer mechanism. This dye can be used as a fluorescent proton sensor following the switch on/off of the fluorescent signal.

In multichromophoric poly–*p*–phenylene–BODIPY systems, the bright visible emission of the BODIPY core can be observed by direct excitation of the poly–*p*–phenylene unit at the UV region via an intramolecular energy transfer process of the excitation energy from the poly–*p*–phenylene unit to the BODIPY moiety. A very high "pseudo" Stokes shift is obtained, which facilities the recorded fluorescence signal in the Vis region without any interference of the scattering of the excitation/pumping light in the UV.

7. Acknowledgements :

Dr. F. Amat-Guerri, Dr. R. Sastre and Dr. I. Garcia- Moreno, from the CSIC (Madrid), are thanked for their collaboration in the synthesis of new BODIPY analogs, the BODIPY-polymer matrices preparation and the BOPDIPY lasing characterization, respectively. The Spanish Education and Science Ministry (MEC: MAT2007-65778-C02-02) and the Basque Country University (UPV/EHU: GIU06-80) are thanked for financial supports in the last few years.

8. References :

[1] M. Maeda, Laser Dyes. (Academic Press, Tokyo, 1984).
[2] F. P. Schäfer, Dye Lasers. (3rd Ed., Springer-Verlag, Berlin, 1990).
[3] A. Prasanna de Silva, H. Q. N. Gunaratne, T. Gunnlaugsson, A. J. M. Huxley, C. P. McCoy, J. T. Rademacher, and T. E. Rice, Chem. Rev. 97 (1997) 1515.
[4] B. Valeur, and I. Leray, Coord. Chem. Rev. 205 (2000) 3.
[5] K. Rurack, and U. Resch-Genger, Chem. Soc. Rev. 31 (2002) 116.
[6] H. Zollinger, Color Chemistry (3rd Ed.,Wiley-VCH, Zurich, 2003).
[7] J. R. Lakowicz, Principles of Fluorescence Spectroscopy (3rd Ed., Springer, Singapore, 2006).
[8] M. Vogel, W. Rettig, R. Sens, and K. H. Drexhage, Chem. Phys. Lett. 147 (1988) 452.
[9] R. Reisfeld, D. Brusilovsky, M. Eyal, E. Miron, Z. Burstein, and J. Ivri, Chem. Phys. Lett. 160 (1989) 43.
[10] F. López Arbeloa, A. Costela, and I. López Arbeloa, J. Photochem. Photobiol. A 55 (1990) 97.
[11] F. López Arbeloa, T. López Arbeloa, and I. López Arbeloa, Trends Photochem. Photobiol. 3 (1994) 145.
[12] T. López Arbeloa, F. López Arbeloa, I. López Arbeloa, A. Costela, I. García-Moreno, J. M. Figuera, F. Amat-Guerri, and R. Sastre, J. Lumin. 75 (1997) 309.
[13] F. López Arbeloa, T. López Arbeloa, I. López Arbeloa, A. Costela, I. García-Moreno, J. M. Figuera, F. Amat-Guerri, and R. Sastre, Appl. Phys. B 64 (1997) 651.
[14] V. N. Serova, V. V. Chirkov, V. I. Morozov, V. V. Semashko, and V. P. Arkhireev, Chem. Trans. 41 (1999) 1409.
[15] J. Huang, V. Bekiari, P. Lianos, and S. Couris, J. Lumin. 81 (1999) 285.

[16] F. López Arbeloa, T. López Arbeloa, and I. López Arbeloa, in Handbook of Advanced Electronic and Photonic Materials and Devices, Edited by H. S. Nalwa (Academic Press, San Diego, 2001).
[17] A. Treibs, and F. H. Kruzer, Justus Liebigs Ann. Chem. 718 (1968) 208.
[18] T. G. Pavlopoulos, M. Shah, and J. H. Boyer, Appl. Opt. 27 (1988) 4998.
[19] M. Shah, K. Thangaraj, M-L. Soong, L. T. Wolford, J. H. Boyer, I. R. Politzer, and T. G. Pavlopoulos, Heteroat. Chem. 1 (1990) 389.
[20] T. G. Pavlopoulos, J. H. Boyer, M. Shah, K. Thangaraj, and M-L. Soong, Appl. Opt. 29 (1990) 3885.
[21] J. H. Boyer, A. M. Haag, G. Sathyamoorthi, M-L. Soong, K. Thangaraj, and T. G. Pavlopoulos, Heteroat. Chem. 4 (1993) 39.
[22] I. D. Johnson, H. C. Kang and R. P. Haugland, Anal. Biochem. 198 (1991) 228.
[23] M. L. Metzker, J. Lu, and R. A. Gibbs, Science 271 (1996) 1420.
[24] S. A. Farber, M. Pack, S-Y. Ho, I. D. Johnson, D. S. Wagner, R. Dosch, M. C. Mullins, H. S. Hendrickson, E. K. Hendrickson, and M E. Halpern, Science 292 (2001) 1385.
[25] R. Reents, M. Wagner, J. Kulhmann, and H. Waldmann, Angew. Chem. Int. Ed. 43 (2004) 2711.
[26] C. Sun, J. Yang, L. Li, X. Wu, Y. Liu, and S. Liu, J. Chromatogr. B 203 (2004) 173.
[27] F. López Arbeloa, J. Bañuelos, V. Martínez, T. Arbeloa, and I. López Arbeloa, Int. Rev. Phys. Chem. 24 (2005) 339.
[28] A. Loudet, and K. Burgess, Chem. Rev. 107 (2007) 4891.
[29] T. E. Wood, and A. Thompson, Chem. Rev. 107 (2007) 1831.
[30] G. Ulrich, R. Ziessel, and A. Harriman, Angew. Chem. Int. Ed. 47 (2008) 1184.
[31] J. Karolin, L. B-A. Johansson, L. Strandberg, and T. Ny, J. Am. Chem. Soc. 116 (1994) 7801.
[32] F. López Arbeloa, T. López Arbeloa, and I. López Arbeloa, Recent Res. Devel. Photochem. Photobiol. 3 (1999) 35.
[33] R. Y. Lai, and A. J. Bard, J. Phys. Chem. B 107 (2003) 5036.
[34] Z. Shen, H. Röhr, K. Rurack, H. Uno, M. Spieles, B. Schulz, G. Reck, and N. Ono, Chem. Eur. J. 10 (2004) 4853.
[35] W. Qin, M. Baruah, M. Van der Auweraer, F. C. De Schryver, and N. Boens, J. Phys. Chem. A 109 (2005) 7371.
[36] A. D. Quartorolo, N. Russo, and E. Sicilia, Chem. Eur. J. 12 (2006) 6797.
[37] S. Badré, V. Monnier, R. Méallet-Renault, C. Dumas-Verdes, E. Y. Schmidt, B. A. Trofimov, and R. B. Pansu, J. Photochem. Photobiol. A 183 (2006) 238.
[38] A. Cui, X. Peng, J. Fan, X. Chen, Y. Wu, and B. Guo, J. Photochem. Photobiol. A 186 (2007) 85.
[39] Y. Assor, Z. Burshtein, and S. Rosenwaks, Appl. Opt. 37 (1998) 4914.
[40] M. S. Mackey, and W. N. Sisk, Dyes and Pigments 51 (2001) 79.
[41] G. Jones II, O. Klueva, S. Kumar, and D. Pacheco, Int. Soc. Opt. Eng. 4267 (2001) 24.
[42] M. D. Rahn and T. A. King, Appl. Opt. 34 (1995) 8260.
[43] A. Dubois, M. Canva, A. Brun, F. Chaput, and J-P. Boilot, Appl. Opt. 35 (1996) 3193.
[44] E. Yariv, S. Schultheiss, T. Saraidarov, and R. Reisfeld, Opt. Mater. 16 (2001) 29.
[45] A. Costela, I. García-Moreno, and R. Sastre, in Handbook of Advanced Electronic and Photonic Materials and Devices, Edited by H. S. Nalwa (Academic Press, San Diego, 2001).
[46] M. Ahmad, T. A. King, D-K. Ko, B. H. Cha, and J. Lee, J. Phys. D 35 (2002) 1473.

[47] A. Costela, I. García-Moreno, and R. Sastre, Phys. Chem. Chem. Phys. 5 (2003) 4745.
[48] M. Alvarez, F. Amat-Guerri, L. Campo, A. Costela, I. García-Moreno, O. García, C. Gómez, C. Gutierrez, M. Liras, and R. Sastre, Recent Res. Devel. Appl. Phys. 7 (2004) 20.
[49] R. K. Lammi, A. Ambroise, T. Balasubramanian, R. W. Wagner, D. F. Bocian, D. Holten, and J. S. Lindsey, J. Am. Chem. Soc. 122 (2000) 7579.
[50] R. K. Lammi, R. W. Wagner, A. Ambroise, J. R. Diers, D. F. Bocian, D. Holten, and J. S. Lindsey, J. Phys. Chem. B 105 (2001) 5341.
[51] H. Imahori, H. Norieda, H. Yamada, Y. Nishimura, I. Yamazaki, Y. Sakata, and S. Fukuzumi, J. Am. Chem. Soc. 123 (2001) 100.
[52] A. Ambroise, C. Kirmaier, R. W. Wagner, R. S. Loewe, D. F. Bocian, D. Holten, and J. S. Lindsey, J. Org. Chem. 67 (2002) 3811.
[53] S. Hattori, K. Ohkubo, Y. Urano, H. Sunhara, T. Pagano, Y. Wada, N. V. Tkachenko, H. Lemmetyinen, and S. Fukuzumi, J. Phys. Chem. B 109 (2005) 15368.
[54] S. Blaya, P. Acebal, L. Carretero, and A. Fimia, Opt. Comun. 228 (2003) 55.
[55] S. Y. Lam, and M. J. Damzen, Opt. Commun. 218 (2003) 365.
[56] R. Jakubiak, L. V. Natarajan, V. Tondiglia, G. S. He, P. N. Prasad, T. J. Bunning, and R. A. Vaia, Appl. Phys. Lett. 85 (2004) 6095.
[57] T. Werner, Ch. Huber, S. Heinl, M. Kollmannsberger, J. Daub, and O. S. Wolfneis, Fresenius J. Anal. Chem. 359 (1997) 150.
[58] M. Baruah, W. Qin, N. Basaric, W. M. De Borggraeve, and N. Boens, J. Org. Chem. 70 (2005) 4152.
[59] M. Baruah, W. Qin, C. Flors, J. Hofkens, R. A. L. Vallée, D. Beljonne, M. Van der Auweraer, W. M. De Borggraeve, and N. Boens, J. Phys. Chem. A 110 (2006) 5998.
[60] H. Sunahara, Y. Urano, H. Kojima, and T. Pagano, J. Am. Chem. Soc. 129 (2007) 5597.
[61] Y. Ando, S. Iino, J. Yamada, K. Umezawa, N. Iwasawa, D. Citterio, and K. Suzuki, Sensors and Actuators B 121 (2007) 74.
[62] K. Rurack, M. Kollmannsberger, U. Resch-Genger, and J. Daub, J. Am. Chem. Soc. 122 (2000) 968.
[63] A. Coskun, B. T. Baytekin, and E. U. Akkaya, Tetrahedron Lett. 44 (2003) 5649.
[64] C. Goze, G. Ulrich, L. Charbonnière, M. Cesario, T. Prangé, and R. Ziessel, Chem. Eur. J. 9 (2003) 3748.
[65] Y. Gabe, Y. Urano, K. Kikuchi, H. Kojima, and T. Nagano, J. Am. Chem. Soc. 126 (2004) 3357.
[66] R. Méallet-Renault, R. Pansu, S. Amigoni-Gerbier, and C. Larpent, Chem. Comm. (2004) 2344.
[67] S. Y. Moon, N. R. Cha, Y. H. Kim, and S-K. Chang, J. Org. Chem. 69 (2004) 181.
[68] H. Koutaka, J. Kosuge, N. Fukasaku, T. Hirano, K. Kikuchi, Y. Urano, H. Kojima, and T. Nagano, Chem. Pharm. Bull. 52 (2004) 700.
[69] J. L. Bricks, A. Kovalchuk, C. Trieflinger, M. Nofz, M. Büschel, A. I. Tomalchev, J. Daub, and K. Rurack, J. Am. Chem. Soc. 127 (2005) 13522.
[70] K. Yamada, Y. Nomura, D. Citterio, N. Iwasawa, and K. Suzuki, J. Am. Chem. Soc. 127 (2005) 6956.
[71] N. Basaric, M. Baruah, W. Qin, B. Metten, M. Smet, W. Dehaen, and N. Boens, Org. Biomol. Chem. 3 (2005) 2755.
[72] T. Kálai, and K. Hideg, Tetrahedron 62 (2006) 10352.

[73] C. Garzillo, R. Improta, and A. Peluso, J. Molec. Struct. 426 (1998) 145.
[74] W. M. F. Fabian, and J. M. Kauffman, J. Lumin 85 (1999) 137.
[75] W. M. F: Fabian, K. S. Niederreiter, G. Uray, and W. Stadlbauer, J. Molec. Struct. 477 (1999) 209.
[76] J-R. Hill, L. Subramanian, and A. Maiti, Molecular Modeling Techniques in Materials Science (Taylor & Francis, Boca Raton, 2005).
[77] H-D. Höltje, W. Sippl, D. Rognan, and G. Folkers, Molecular Modeling (Wiley-VCH, Weinheim, 2008)
[78] F. López Arbeloa, T. López Arbeloa, I. López Arbeloa, I. García-Moreno, A. Costela, R. Sastre, and F. Amat-Guerri, Chem. Phys. 236 (1998) 331.
[79] J. Bañuelos, F. López Arbeloa, V. Martínez, and I. López Arbeloa, Chem. Phys. 296 (2004) 13.
[80] T . G. Pavlopoulos, Prog. Quantum Elect. 26 (2002) 193.
[81] A. A. Gorman, I. Hamblett, T. A. King, and M. D. Rahn, J. Photochem. Photobiol. 130 (2000) 127.
[82] Y-H. Yu, Z. Shen, H-Y. Xu, Y-W. Wang, T. Okujima, N. Ono, Y-Z. Li, and X-Z. You, J. Molec. Struct. 827 (2007) 130.
[83] J. Bañuelos, F. López Arbeloa, V. Martínez, T. Arbeloa López, F. Amat-Guerri, M Liras, and I. López Arbeloa, Chem. Phys. Lett. 385 (2004) 29.
[84] A. Costela, I. García-Moreno, C. Gómez, R. Sastre, F. Amat-Guerri, M. Liras, F. López Arbeloa, J. Bañuelos, and I. López Arbeloa, J. Phys. Chem. A 106 (2002) 7736.
[85] I. López Arbeloa, J. Photochem. 14 (1980) 97.
[86] F. López Arbeloa T. López Arbeloa, and I. López Arbeloa, J. Photochem. Photobiol. A 121 (1999) 177.
[87] J. Bañuelos, F. López Arbeloa, V. Martínez. T. Arbeloa López, and I. López Arbeloa, J. Phys. Chem. A 108 (2004) 5503.
[88] J. Bañuelos, F. López Arbeloa, V. Martínez, T. Arbeloa López, and I. López Arbeloa, Phys. Chem. Chem. Phys. 6 (2004) 4247.
[89] J. Fabian, and H. Hartmann, Light Absorption of Organic Colorants (Springer-Verlag, Berlin, 1980).
[90] N. Tyultyulkov, J. Fabian, A. Mehlhorn, F. Dietz, and A. Tadjer, Polymethine Dyes (Jusautor, Sofia, 1991).
[91] Y. Marcus, Chem. Soc. Rev. 22 (1993) 409.
[92] A. R. Katritzky, D. C. Fara, H. Yang, K. Tämm, T. Tamm and M. Karelson, Chem. Rev. 104 (2004) 175.
[93] M. J. Kamlet, and R. W. Taft, J. Am. Chem. Soc. 98 (1976) 377.
[94] M. J. Kamlet, and R. W. Taft, J. Am. Chem. Soc. 98 (1976) 2886.
[95] M. J. Kamlet, J. L. M. Abboud, and R. W. Taft, J. Am. Chem. Soc. 99 (1977) 6027.
[96] C. Reichardt, Chem. Rev. 94 (1994) 2319.
[97] T. López Arbeloa, F. López Arbeloa, I. López Arbeloa, I. García-Moreno, A. Costela, R. Sastre and F. Amat-Guerri, Chem. Phys. Lett. 299 (1999) 315.
[98] A. Costela, I. García-Moreno, J. M. Figuera, F. Amat-Guerri, and R. Sastre, Laser Chem. 18 (1998) 63.
[99] F. López Arbeloa, J. Bañuelos, I. López Arbeloa, A. Costela, I. García-Moreno, C. Gómez, F. Amat-Guerri, M. Liras, and R. Sastre, Photochem. Photobiol. 78 (2003) 30.
[100] I. García-Moreno, A. Costela, L. Campo, R. Sastre, F. Amat-Guerri, M. Liras, F. López Arbeloa, J. Bañuelos, and I. López Arbeloa, J. Phys. Chem. A 108 (2004) 3315.

[101] J. Bañuelos, F. López Arbeloa, O. García, and I. López Arbeloa, J. Lumin. 126 (2007) 833.
[102] I. García-Moreno, F. Amat-Guerri, M. Liras, A. Costela, L. Infantes, R. Sastre, F. López Arbeloa, J. Bañuelos, and I. López Arbeloa, Adv. Funct. Mater. 17 (2007) 3088.
[103] O. García, R. Sastre, D. del Agua, A. Costela, I. García-Moreno, F. López Arbeloa, J. Bañuelos, and I. López Arbeloa, J. Phys. Chem. C 111 (2007) 1508.
[104] A. Costela, I. García-Moreno, C. Gómez, O. García, and R. Sastre, J. Appl. Phys. 90 (2001) 3159.
[105] F. Li, S. I. Yang, Y. Ciringh, J. Seth, C. H. Martin III, D. L. Singh, D. Kim, R. R. Birge, D. F. Bocian, D. Holten, and J. S. Lindsey, J. Am. Chem. Soc. 120 (1998) 10001.
[106] H. Kim, A. Burghart, M. B. Welch, J. Reibenspies, and J. Burgess, Chem. Commun. (1999) 1889.
[107] J. Chen, A. Burghart, A. Dercskei-Kovacs, and K. Burgess, J. Org. Chem. 65 (2000) 2900.
[108] H. L. Kee, C. Kirmaier, L. Yu, P. Thamyongkit, W. J. Youngblood, M. E. Calder, L. Ramos, B. C. Noll, D. F. Bocian, W. R. Scheidt, R. R. Birge, J. S. Lindsey, and D. Holten, J. Phys. Chem. B 109 (2005) 20433.
[109] G. Jones II, Z. Huang, S. Kumar, and D. Pacheco, Int. Soc. Opt. Eng. 4630 (2002) 72.
[110] G. Jones II, Z. Huang, and D. Pacheco, Int. Soc. Opt. Eng. 4968 (2003) 24.
[111] T. Rohand, W. Qin, N. Boens, and W. Dehaen, Eur. J. Org. Chem. (2006) 4658.
[112] A. Harriman, L. J. Mallon, S. Goeb, and R. Ziessel, Phys. Chem. Chem. Phys. 9 (2007) 5199.
[113] A. Wakamiya, N. Sugita, and S. Yamaguchi, Chem. Lett. 37 (2008) 1094.
[114] K. Umezawa, Y. Nakamura, H. Makino, D. Citterio, and K. Suzuki, J. Am. Chem. Soc. 10 (2008) 1550.
[115] A. Costela, I. García-Moreno, M. Pintado, F. Amat-Guerri, M. Liras, R. Sastre, F. López Arbeloa, J. Bañuelos, and I. López Arbeloa, J. Photochem. Photobiol. 198 (2008) 192.
[116] M. Liras, J. Bañuelos, M. Pintado, F. López Arbeloa, I. García-Moreno, A. Costela, L. Infantes, R. Sastre, and F. Amat-Guerri, Org. Lett. 9 (2007) 4183.
[117] J. Bañuelos, F. López Arbeloa, T. Arbeloa, S. Salleres, J. L. Vilas, F. Amat-Guerri, M. Liras, and I. López Arbeloa, J. Fluoresc. 18 (2008) 899.
[118] R. Reisfeld, E. Yariv, and H. Minti, Opt. Mater. 8 (1997) 31.
[119] M. Alvarez, A. Costela, I. García-Moreno, F. Amat-Guerri, M. Liras, R. Sastre, F. López Arbeloa, J. Bañuelos, and I. López Arbeloa, Photochem. Photobiol. Sci. 7 (2008) 802.
[120] J. Bañuelos, F. López Arbeloa, T. Arbeloa, S. Salleres, F. Amat-Guerri, M. Liras, and I. López Arbeloa, J. Phys. Chem. A 112 (2008) 10816.
[121] S. Speiser, Chem. Rev. 96 (1996) 1953.
[122] T. Förster, Ann. Phys. 2 (1948) 55.
[123] T. Förster, in Modern Quantum Chemistry, Edited by O. Sinanoglu (Academic Press, New York, 1968).
[124] D. L. Dexter, Chem. Phys. 21 (1953) 836.
[125] M. N. Paddon-Row, Acc. Chem. Res. 15 (1982) 245.
[126] R. Gleiter, and W. Schäfer, Acc. Chem. Res. 23 (1990) 369.

[127] G. D. Scholes, K. P. Ghiggino, A. M. Oliver, and M. N. Paddon-Row, J. Phys. Chem. 97 (1993) 11871.
[128] G. D. Scholes, K. P. Ghiggino, A. M. Oliver, and M. N. Paddon-Row, J. Am. Chem. Soc. 115 (1993) 4345.
[129] A. Burghart, L. H. Thoresen, J. Chen, K Burgess, F. Bergström, and L. B-A. Johansson, Chem. Commun. (2000) 2203.
[130] C-W. Wan, A. Burgahrt, J. Chen, F. Bergström, L. B-A. Johansson, M. F: Wolford, T. G. Kim, M. R. Topp, R. M. Hochtrasser, and K. Burgess, Chem. Eur. J. 9 (2003) 4430.
[131] F. D'Souza, P. M. Smith, M. E. Zandler, A. Y. McCarty, M. Itou, Y. Araki, and O. Ito, J. Am. Chem. Soc. 126 (2004) 7898.
[132] D. Kumaresan, A. Datta, and M. Ravikanth, Chem. Phys. Lett. 395 (2004) 87.
[133] G. Ulrich, C. Goze, M. Guardigli, A. Roda, and R. Ziessel, Angew. Chem. Int. Ed. 44 (2005) 3694.
[134] R. Ziessel, C. Goze, G. Ulrich, M. Césario, P. Retailleau, A. Harriman, and J. P. Rostron, Chem. Eur. J. 11 (2005) 7366.
[135] C. Goze, G. Ulrich, and R. Ziessel, J. Org. Chem. 72 (2007) 313.
[136] A. Harriman, G. Izzet, and R. Ziessel, J. Am. Chem. Soc. 128 (2006) 10231.
[137] M. A. H. Alamiry, A. Harriman, L. J. Mallon, G. Ulrich, and R. Ziessel, Eur. J. Org. Chem. (2008) 2774.
[138] F. López Arbeloa, J. Bañuelos, V. Martínez, T. Arbeloa, and I. López Arbeloa, ChemPhysChem 5 (2004) 1762.
[139] Z. R. Grabowski, K. Rotkiewicz, and W. Rettig, Chem. Rev. 103 (2003) 3899.
[140] J. Bañuelos, T. Arbeloa, M. Liras, V. Martínez, and F. López Arbeloa, J. Photochem. Photobiol. A 184 (2006) 298.
[141] A. Korkin, F. Mark, K. Schaffner, L. Gorb, and J. Leszczynski, J. Molec. Struct. 388 (1996) 121.
[142] L. Gorb, A. Korkin, and J. Leszczynski, J. Molec. Struct. 454 (1998) 217.
[143] T. Drapala, Rocz. Chem. 44 (1970) 61.
[144] M. P. O'Neil, Opt. Lett. 18 (1993) 37.